Supporting Information

Poly(cyclodextrin)-Polydrug Nanocomplexes as Synthetic Oncolytic Virus for Locoregional Melanoma Chemoimmunotherapy

*Jihoon Kim, Lauren F. Sestito, Sooseok Im, Won Jong Kim, Susan N. Thomas**

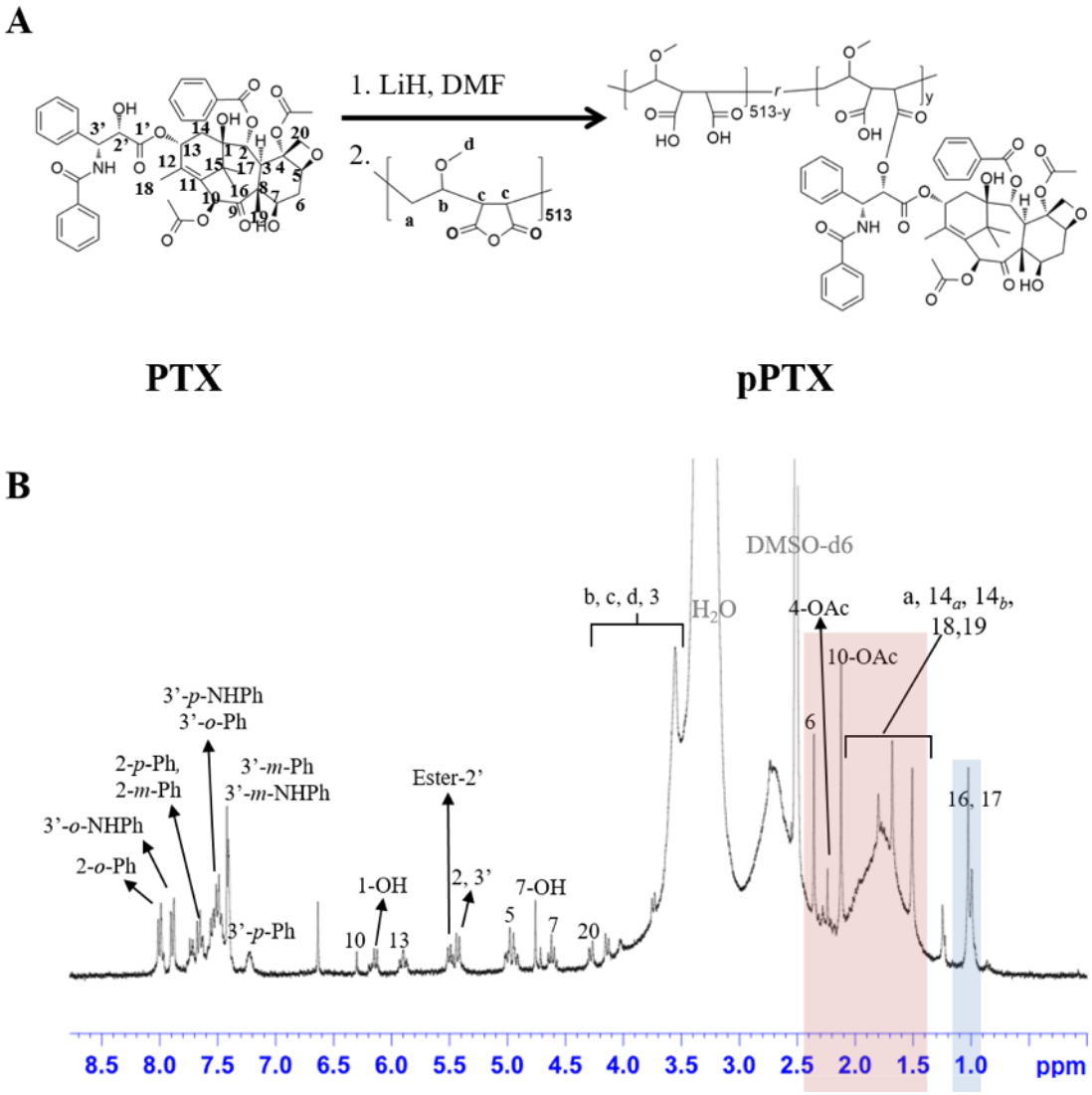

Figure S1. ^{1}H NMR spectra (DMSO-d$_6$, 300 MHz) of pPTX. (A) Synthetic scheme for pPTX. (B) Conjugation ratio of pPTX was calculated by comparing the integration value of PTX (blue box) with that of PTX and poly(methyl vinyl ether-*alt*-Maleic anhydride) (red box).

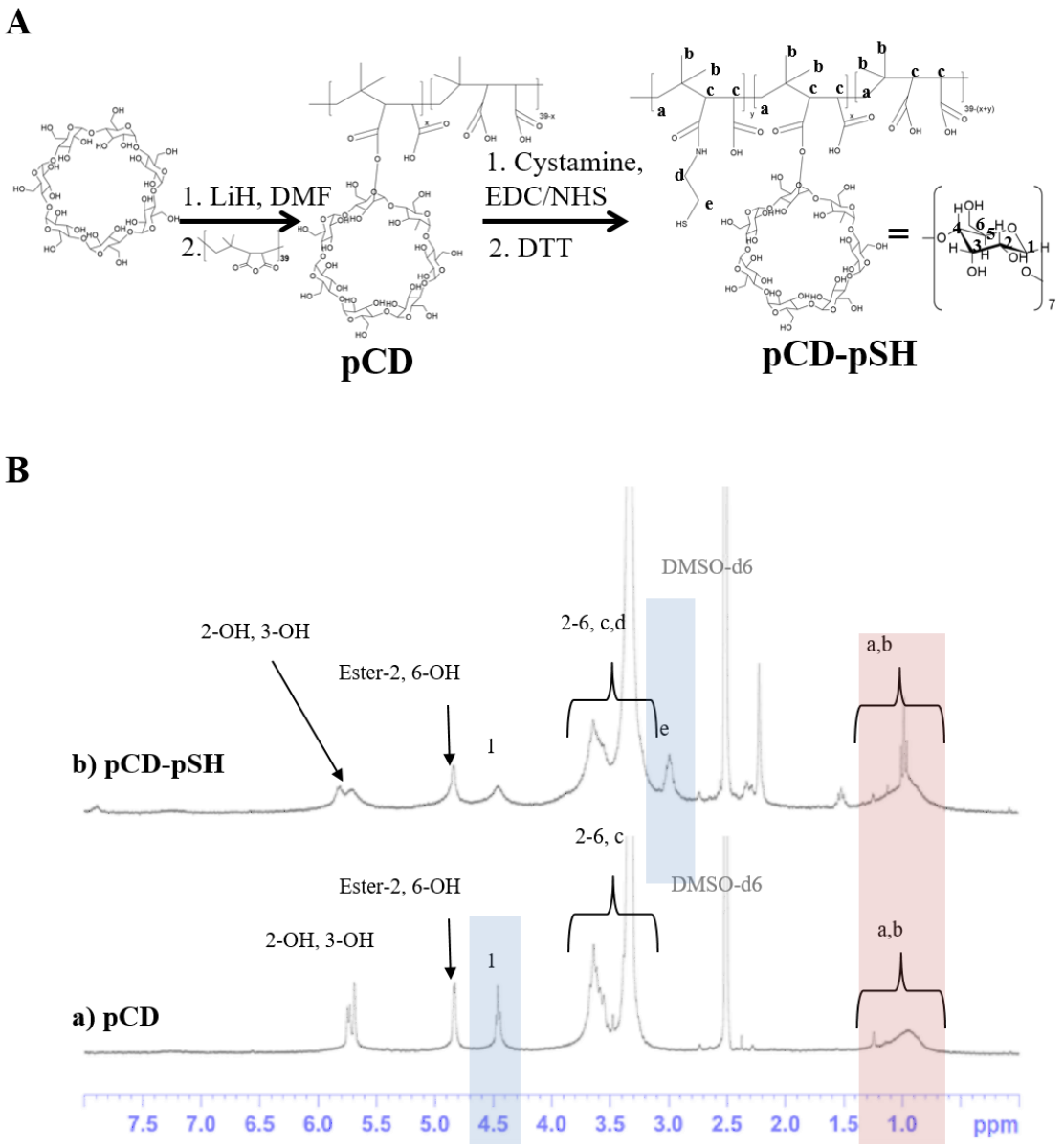

Figure S2. ^{1}H NMR spectra (DMSO-d$_6$, 300 MHz) of pCD and pCD-pSH. (A) Synthetic scheme for pCD-pSH. (B-a) Conjugation ratio of pCD was calculated by comparing the integration value of CD (blue box) with that of poly(isobutylene-*alt*-maleic anhydride) (red box). (B-b) Conjugation ratio of cysteamine in pCD-pSH was calculated by comparing the integration value of cysteamine (blue box) with that of poly(isobutylene-*alt*-maleic anhydride) (red box).

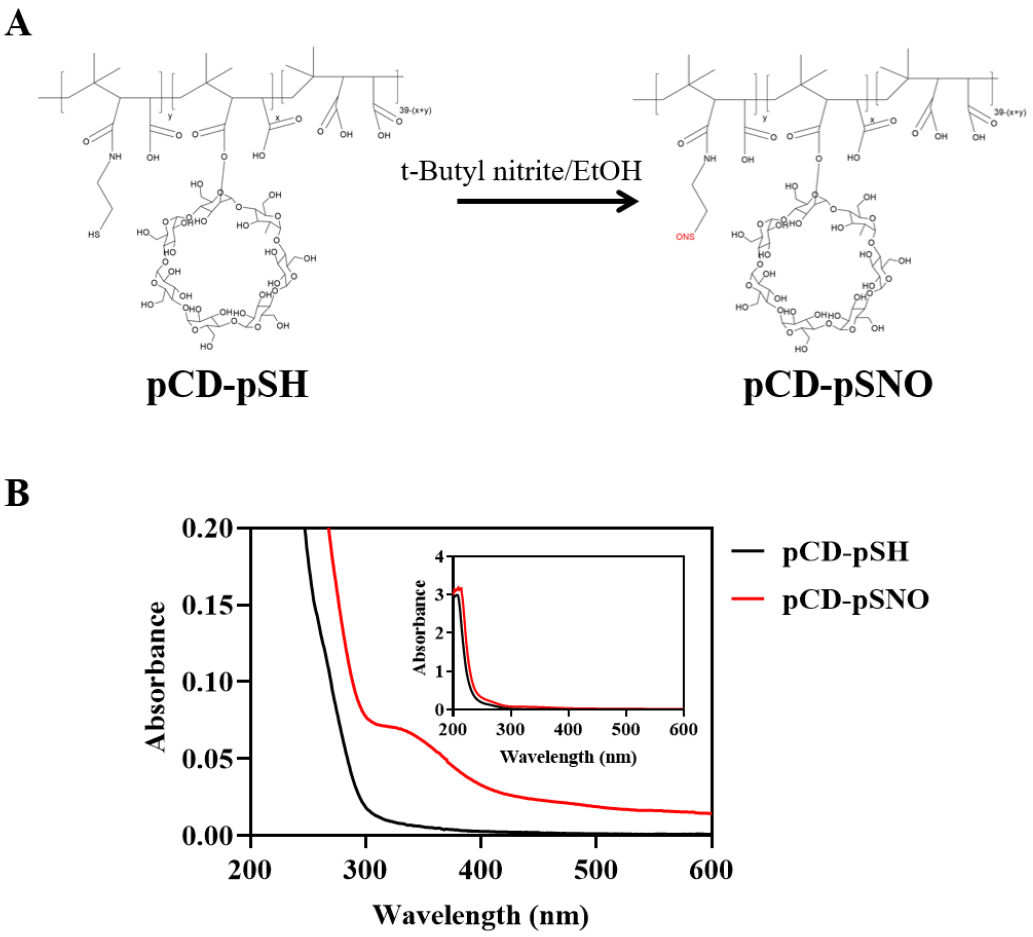

Figure S3. Confirmation of pCD-pSNO. (A) Synthetic scheme for pCD-pSNO. (B) Absorbance of pCD-pSNO in UV-vis spectroscopy.

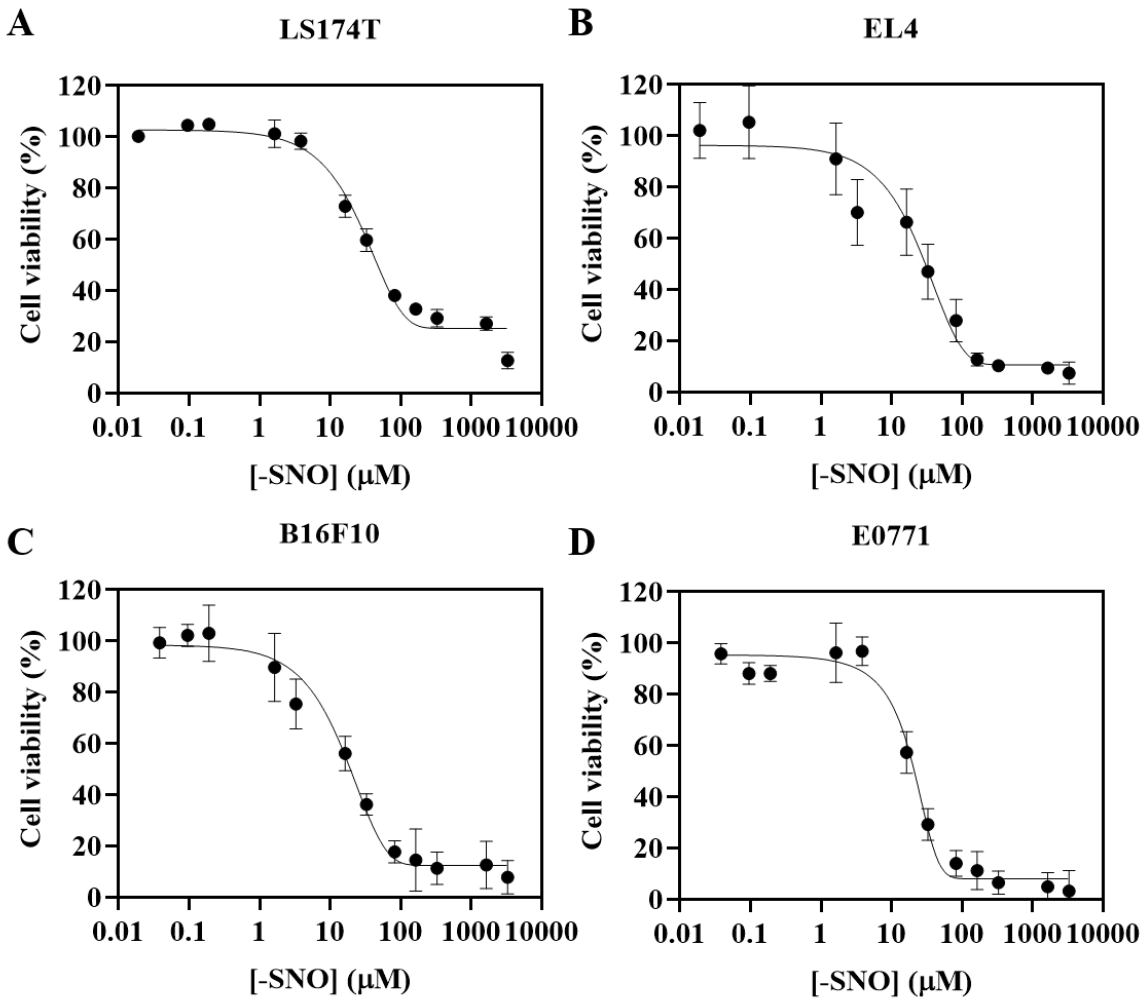

Figure S4. Cytotoxicity test of GSNO. Dose-dependent cytotoxicity of GSNO in (A) LS174T, (B) EL4, (C) B16F10, and (D) E0771 cell lines.

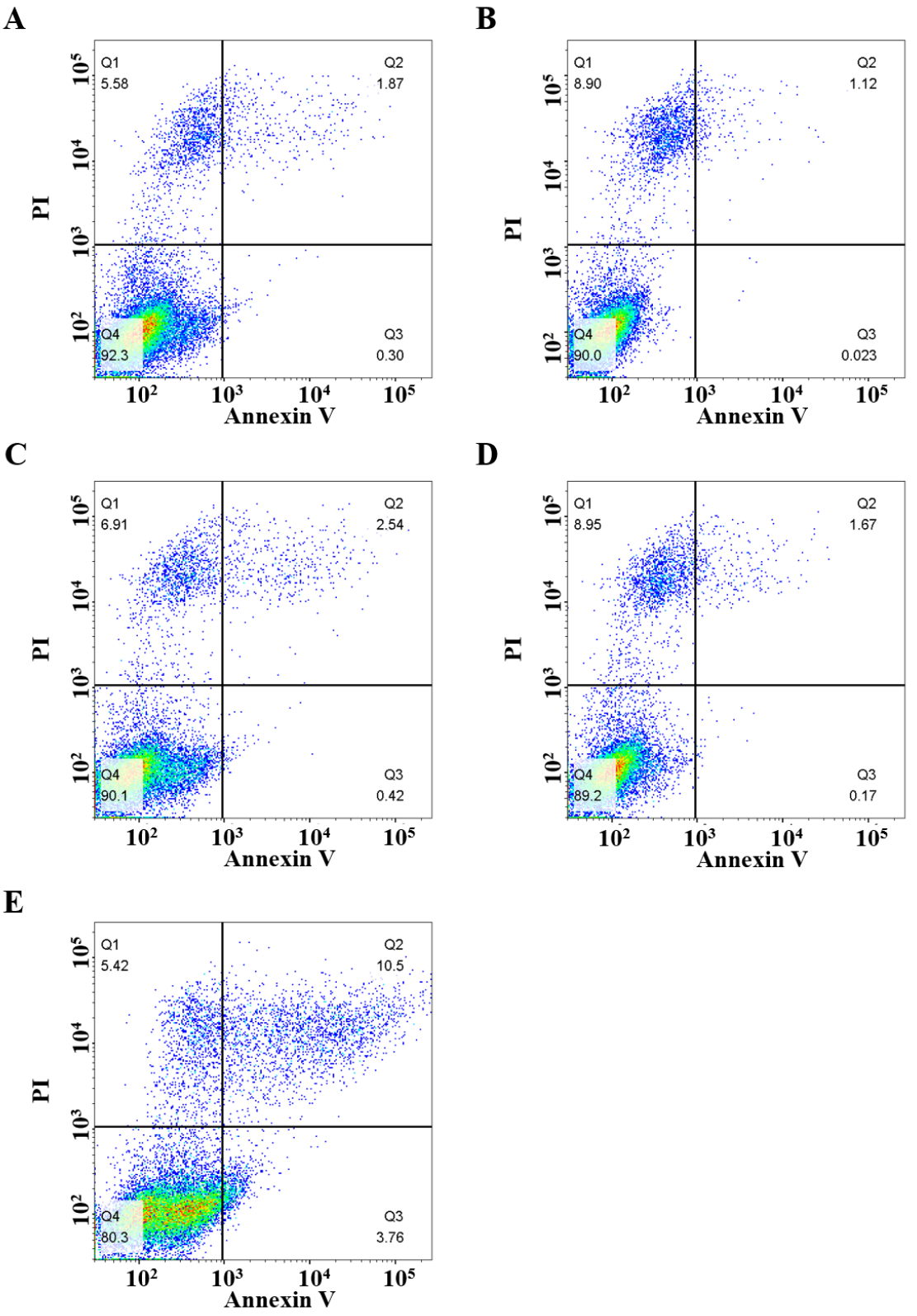

Figure S5. Annexin V/PI assay. (A) PBS, (B) GSNO, (C) PTX, (D) pPTX/pCD-pSH, and (E) pPTX/pCD-pSNO.

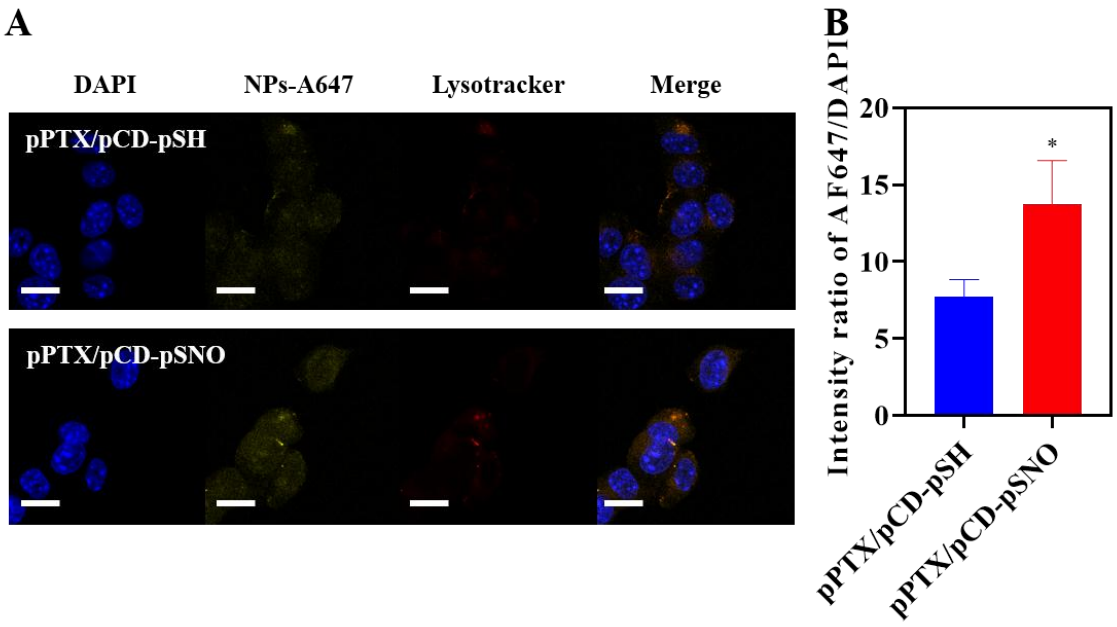

Figure S6. Uptake of NPs. (A) CLSM images of AlexaFluor647-labelled pPTX/pCD-pSH and pPTX/pCD-SNO (yellow) in B16F10 ([PTX] = 1 μM, [-SNO] = 144.5 nM, 4 h incubation). DAPI and lysotracker are shown as blue and red color, respecrively. Scale bar is 20 μm. (B) Quantification of NPs by normalizing the fluorescence intensity of Alexa Fluor™ on NPs with the intensity of DAPI. **p*<0.05.

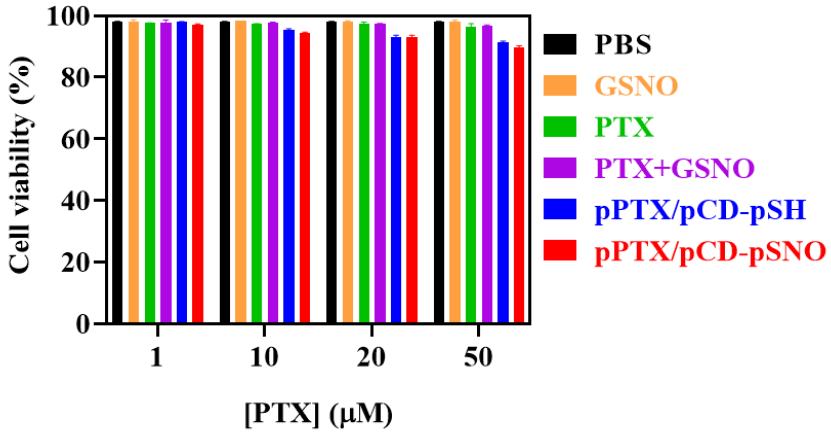

Figure S7. Cytotoxicity of pPTX/pCD-pSNO NPs on BMDCs *in vitro*. Dose dependent viability of BMDCs *in vitro*, evaluated by Live/dead.

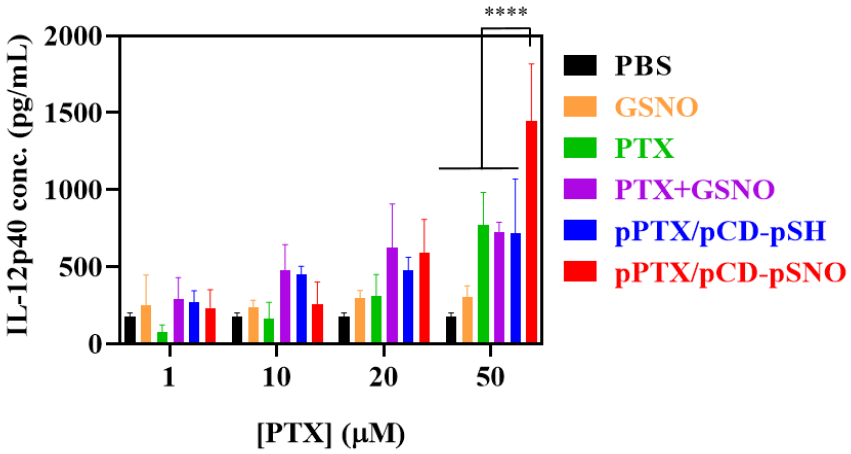

Figure S8. The effects of pPTX/pCD-pSNO NPs on BMDCs *in vitro*. Dose dependent *in vitro* cytokine production of BMDCs, evaluated by IL-12p40.

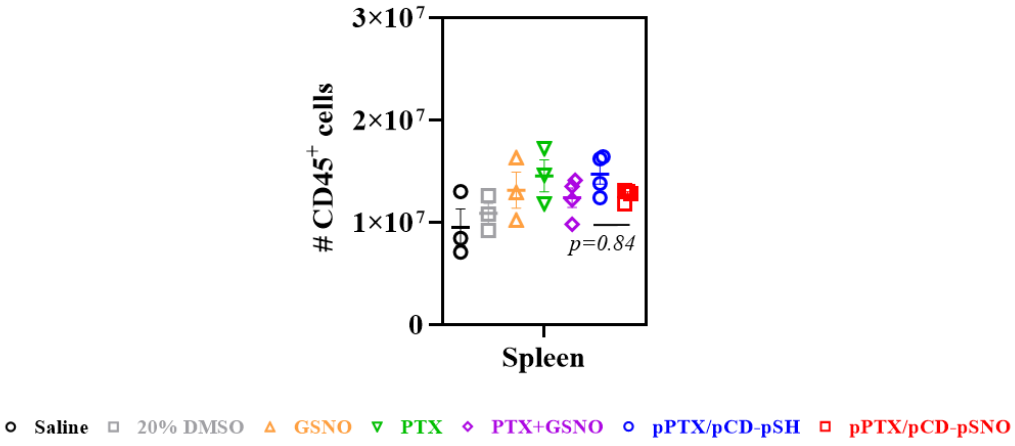

Figure S9. Number of $CD45^+$ cells in spleen 1 d after dorsal injection into tumor-free mouse (C57BL/6J).

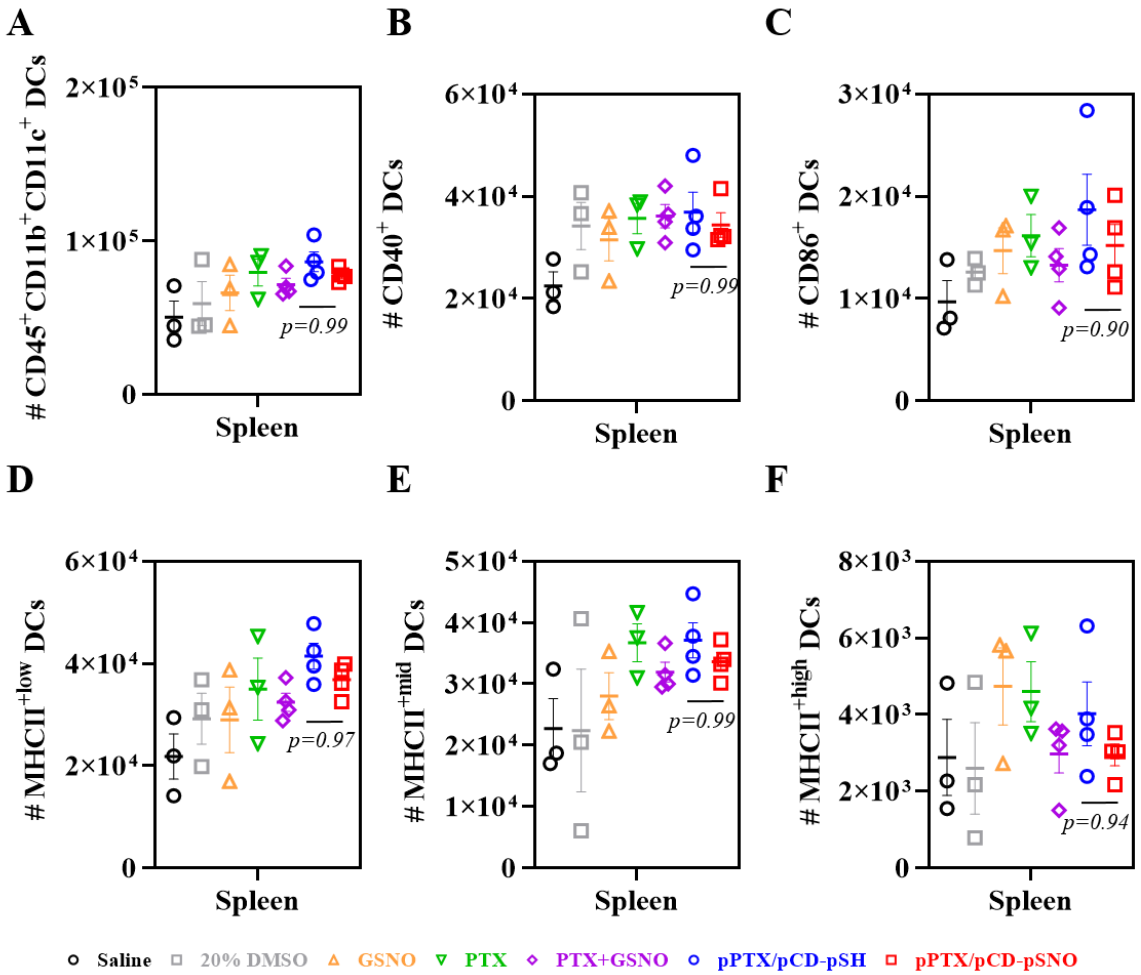

Figure S10. Number profiles of DCs in spleen. Number of (A) $CD45^+CD11b^+CD11c^+$ DCs, (B) $CD40^+$ $CD45^+CD11b^+CD11c^+$ DCs, (C) $CD86^+$ $CD45^+CD11b^+CD11c^+$ DCs, (D) $MHCII^{+low}$ $CD45^+CD11b^+CD11c^+$ DCs, (E) $MHCII^{+mid}$ $CD45^+CD11b^+CD11c^+$ DCs, and (F) $MHCII^{+high}$ $CD45^+CD11b^+CD11c^+$ DCs in spleen 1 d after dorsal injection into tumor-free mouse (C57BL/6J).

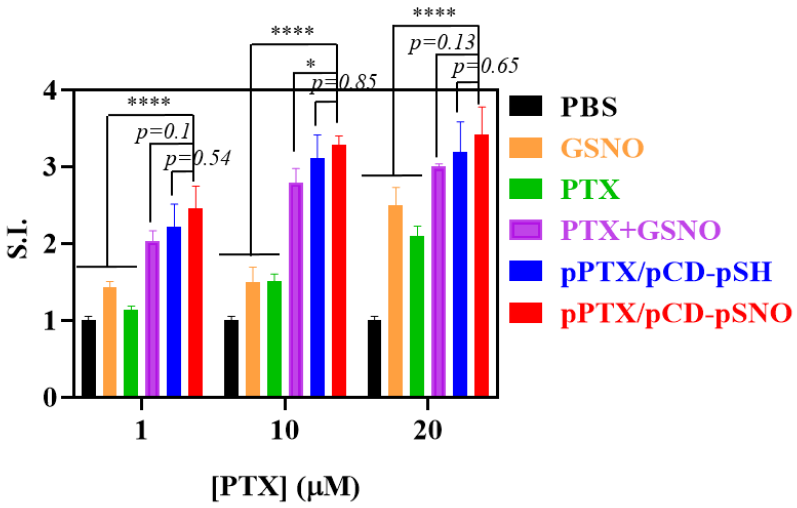

Figure S11. Mixed lymphocytes reactions (MLR) of pPTX/pCD-pSNO NPs. Effects of pPTX/pCD-pSNO NPs on mitomycin C-treated splenocytes (from BALB/c mouse) to stimulate allogeneic T-cell (from C57BL/6J mouse). S.I. means stimulation index.

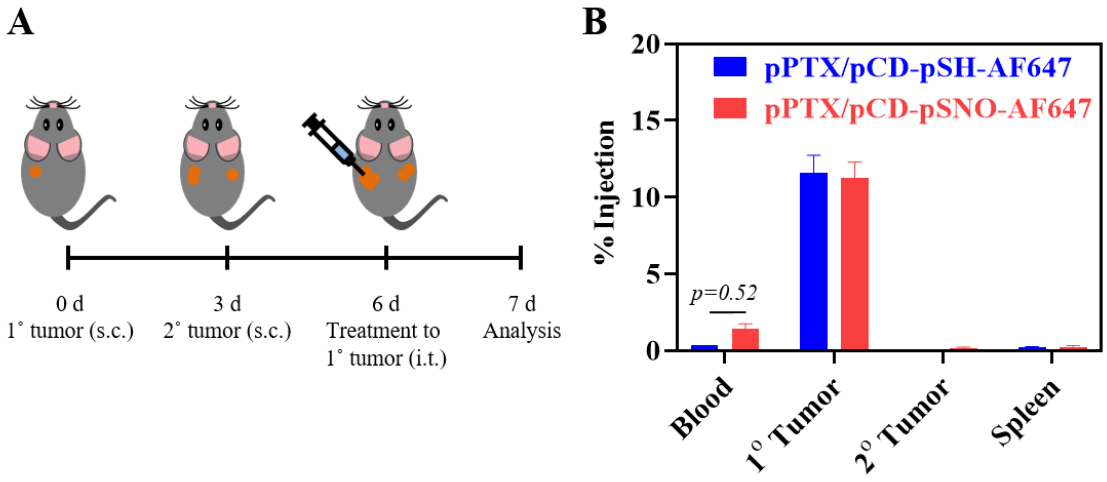

Figure S12. Quantification of nanoparticles in primary and secondary tumor after intratumoral injection in the primary tumor. (A) Schematic schedule to investigate the biodistribution of AlexaFluor647-labelled nanoparticles 24 h after intratumoral injection into primary tumor. (B) Quantification of AlexaFluor647 fluorescence in blood, primary tumor and secondary tumor.

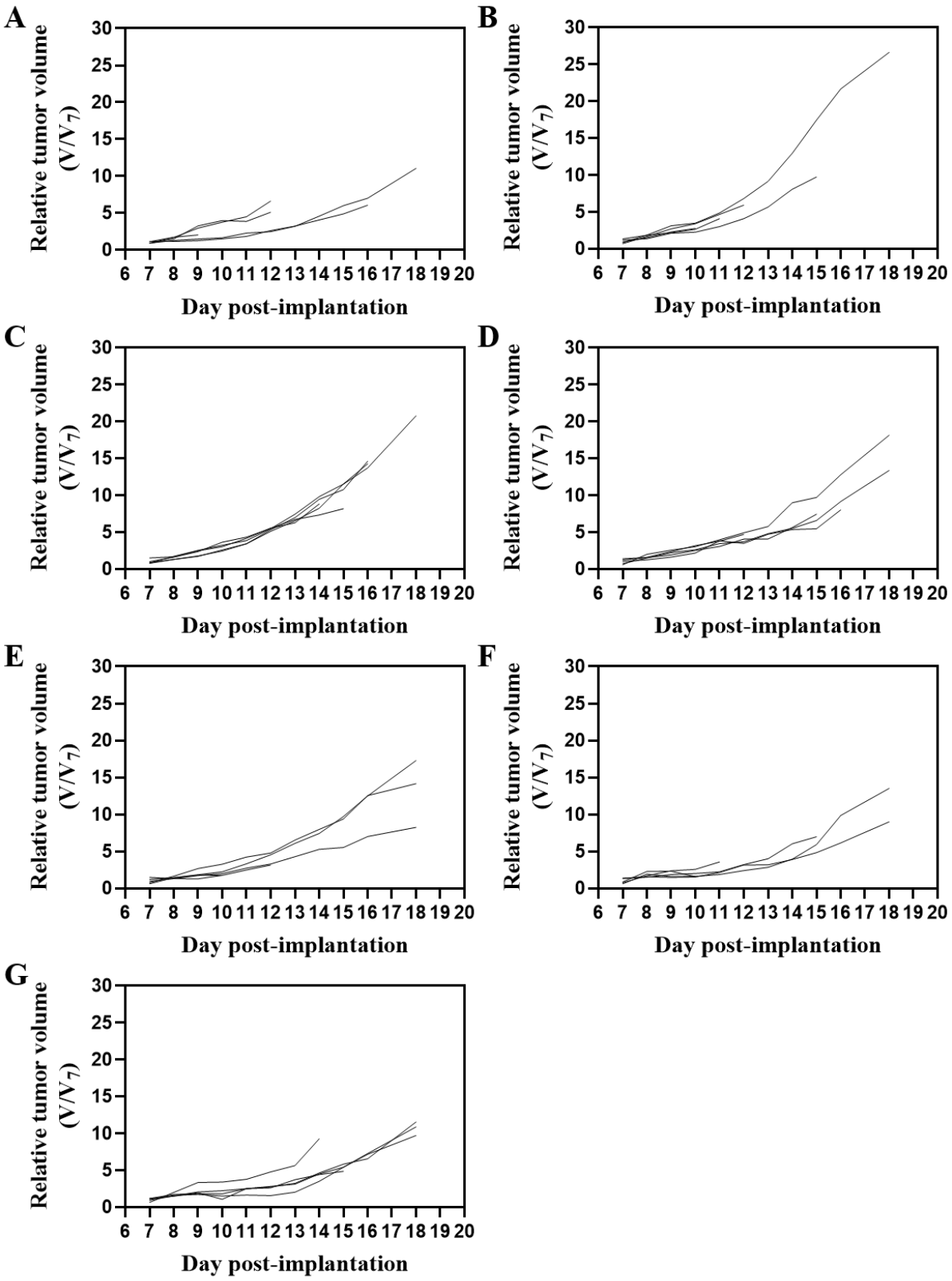

Figure S13. Individual primary tumor size of (A) Saline, (B) DMSO, (C) GSNO, (D) PTX, (E) PTX+GSNO, (F) pPTX/pCD-pSH, and (G) pPTX/pCD-pSNO.

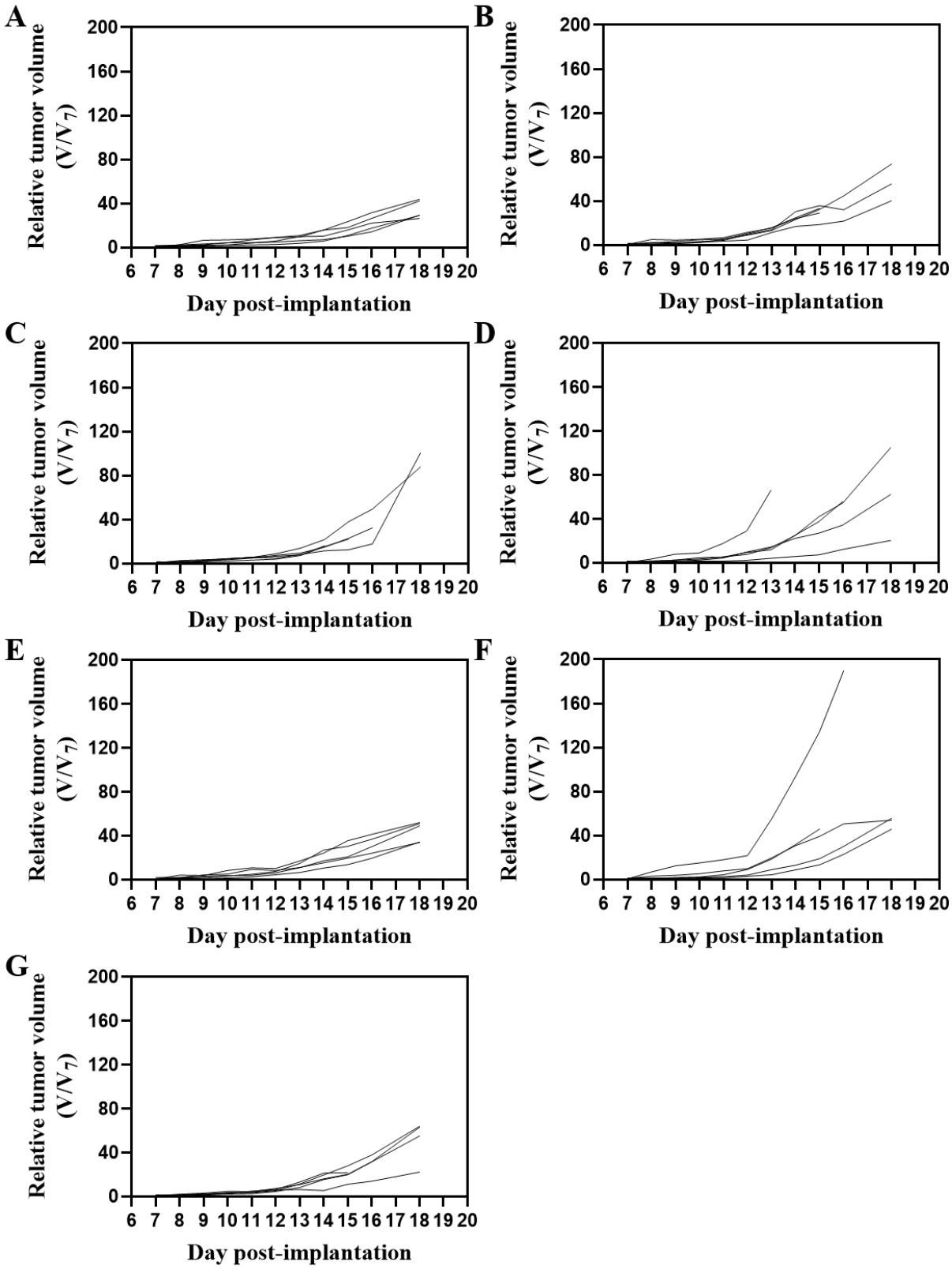

Figure S14. Individual secondary tumor size of (A) Saline, (B) DMSO, (C) GSNO, (D) PTX, (E) PTX+GSNO, (F) pPTX/pCD-pSH, and (G) pPTX/pCD-pSNO.

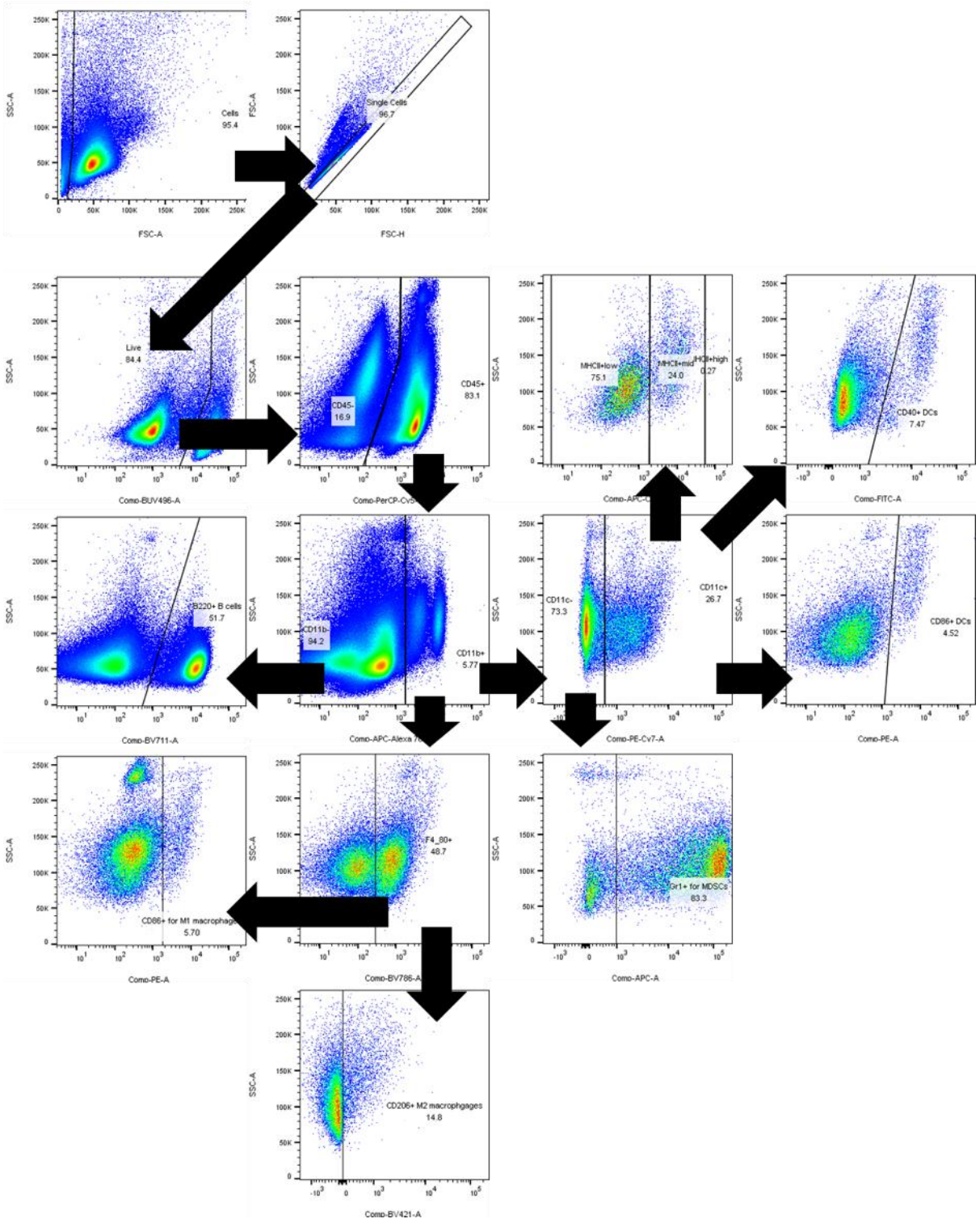

Figure S15. Gating strategy for DCs, macrophages, MDSCs, and B cells.

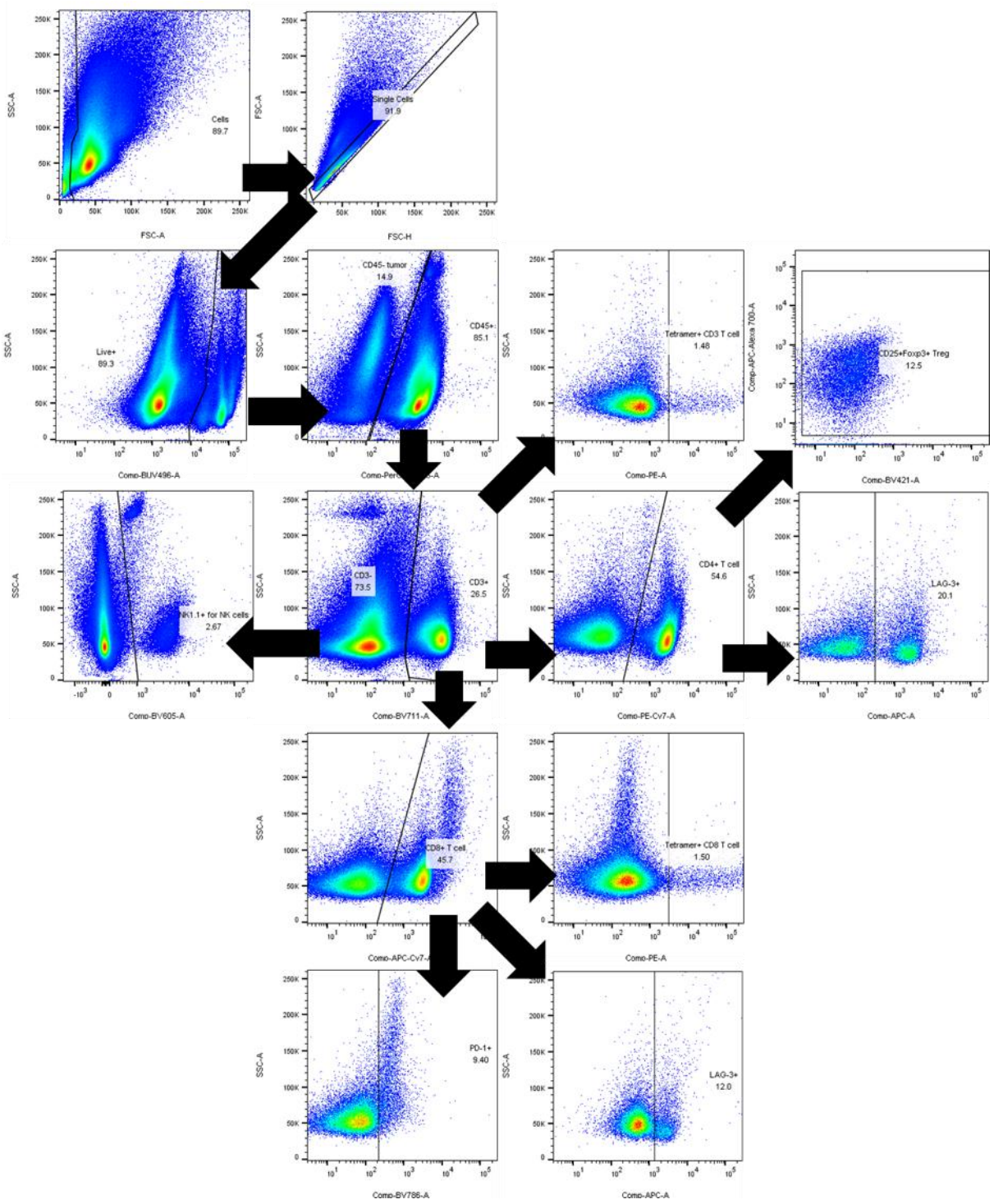

Figure S16. Gating strategy for T cells and NK cells.

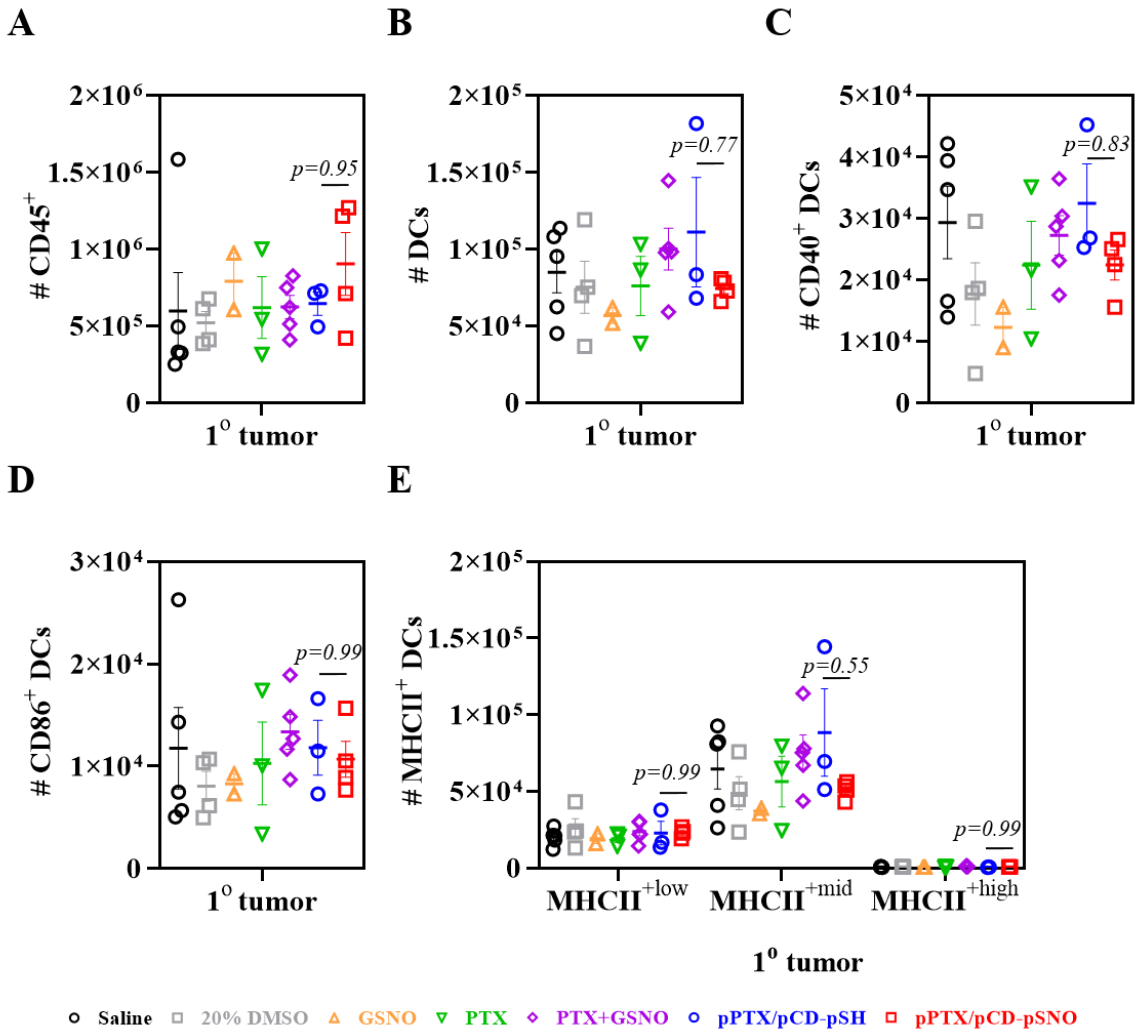

Figure S17. Number profiles of CD45$^+$ cells and DCs in 1^o tumor. Number of (A) CD45$^+$ cells, (B) CD45$^+$CD11b$^+$CD11c$^+$ DCs, (C) CD40$^+$ CD45$^+$CD11b$^+$CD11c$^+$ DCs, (D) CD86$^+$ CD45$^+$CD11b$^+$CD11c$^+$ DCs, (E) MHCII^{+low}, MHCII^{+mid}, and MHCII^{+high} CD45$^+$CD11b$^+$CD11c$^+$ DCs in 1^o tumor.

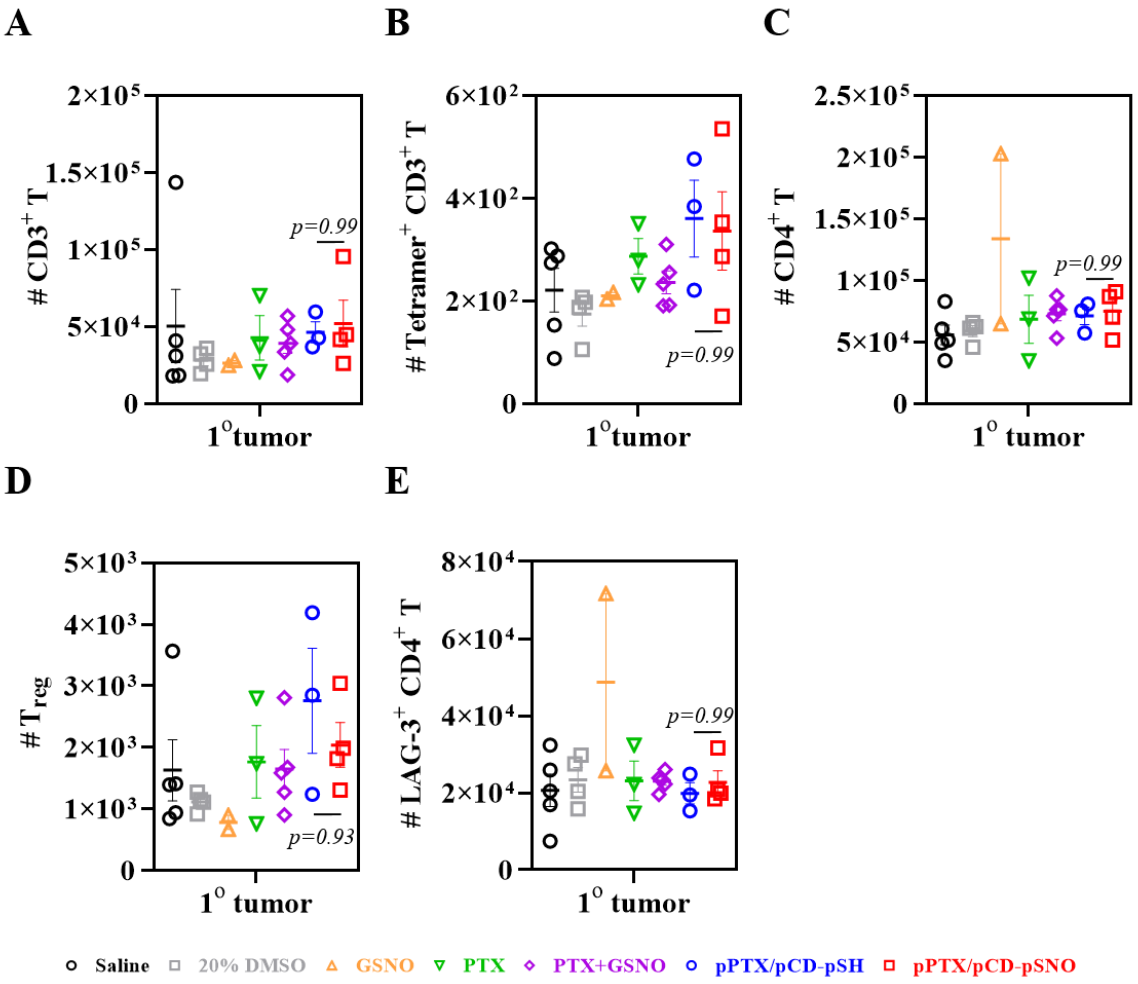

Figure S18. Number profiles of CD3$^+$ T and CD4$^+$ T in 1^o tumor. Number of (A) CD45$^+$CD3$^+$ T cells, (B) Tetramer$^+$ CD45$^+$CD3$^+$ T cells, (C) CD45$^+$CD3$^+$CD4$^+$ T cells, (D) CD45$^+$CD3$^+$CD4$^+$CD25$^+$Foxp3$^+$ T_{reg}, and (E) LAG-3$^+$ CD45$^+$CD3$^+$CD4$^+$ T cells in 1^o tumor.

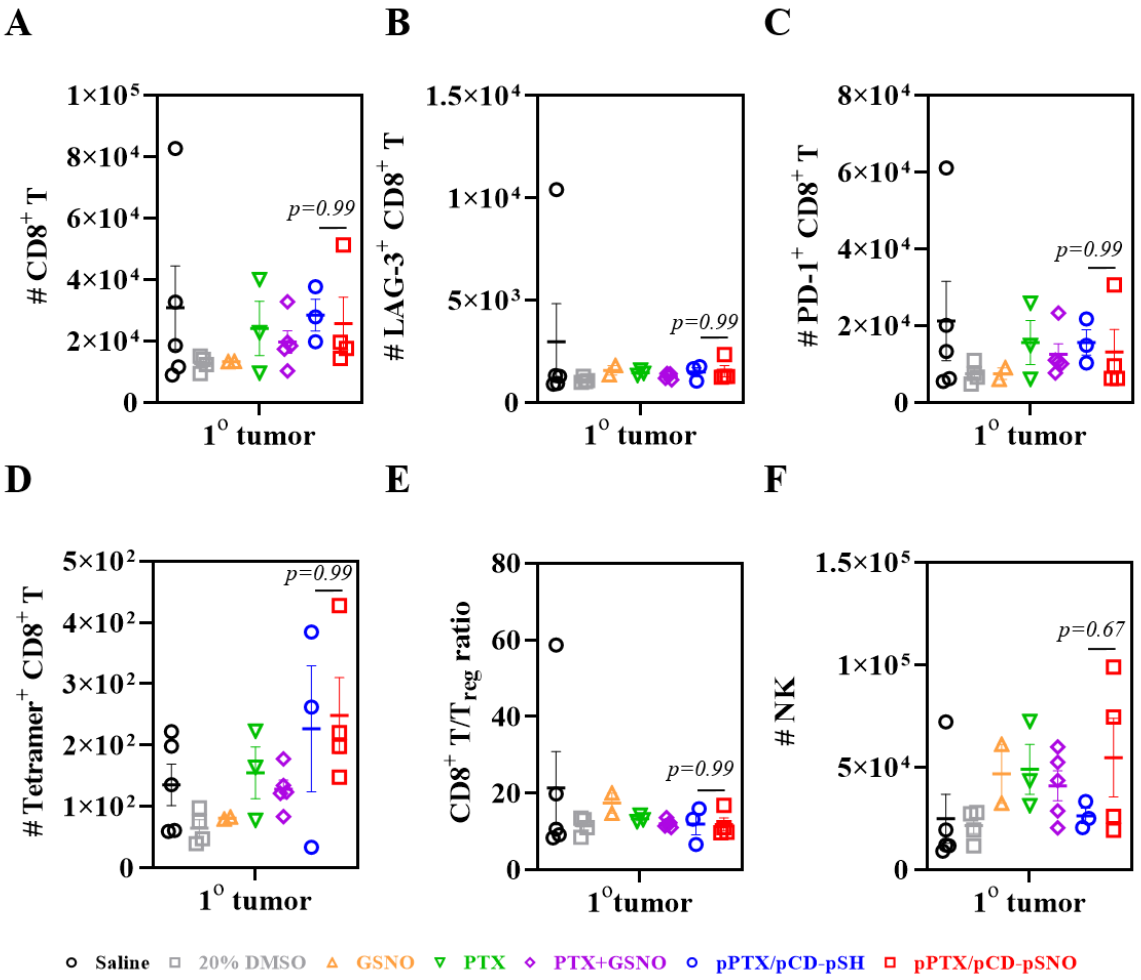

Figure S19. Number profiles of CD8$^+$ T and NK cells in 1^o tumor. Number of (A) CD45$^+$CD3$^+$CD8$^+$ T cells, (B) LAG-3$^+$ CD45$^+$CD3$^+$CD8$^+$ T cells, (C) PD-1$^+$ CD45$^+$CD3$^+$CD8$^+$ T cells, (D) Tetramer$^+$ CD45$^+$CD3$^+$CD8$^+$ T cells, (E) ratio of CD8$^+$ T cells to T_{reg}, and (F) CD45$^+$CD3$^-$NK1.1$^+$ NK cells in 1^o tumor.

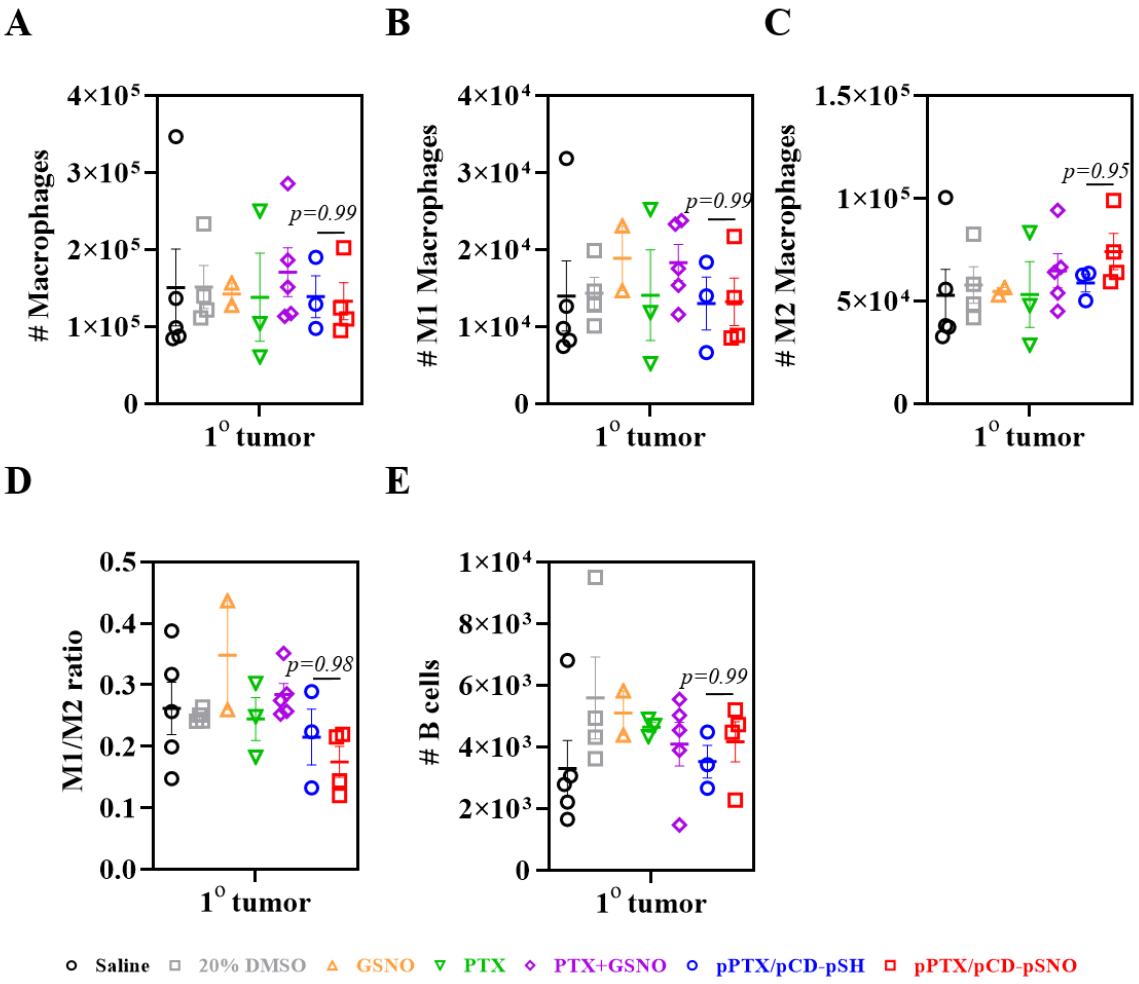

Figure S20. Number profiles of macrophages, and B cells in 1° tumor. Number of (A) $CD45^+CD11b^+F4/80^+$ macrophages, (B) $CD45^+CD11b^+F4/80^+CD86^+$ M1 macrophages, (C) $CD45^+CD11b^+F4/80^+CD206^+$ M2 macrophages, (D) ratio of M1 to M2, and (E) $CD45^+CD11b^-B220^+$ B cells in 1° tumor.

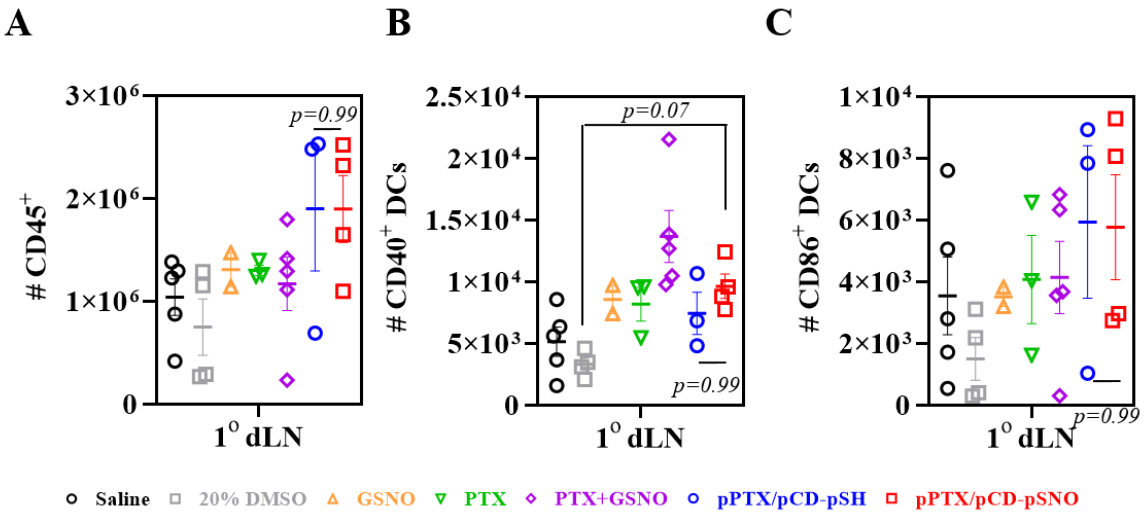

Figure S21. Number profiles of CD45$^+$ cells and DCs in 1º dLN. Number of (A) CD45$^+$ cells, (B) CD40$^+$ CD45$^+$CD11b$^+$CD11c$^+$ DCs, and (C) CD86$^+$ CD45$^+$CD11b$^+$CD11c$^+$ DCs in 1º dLN.

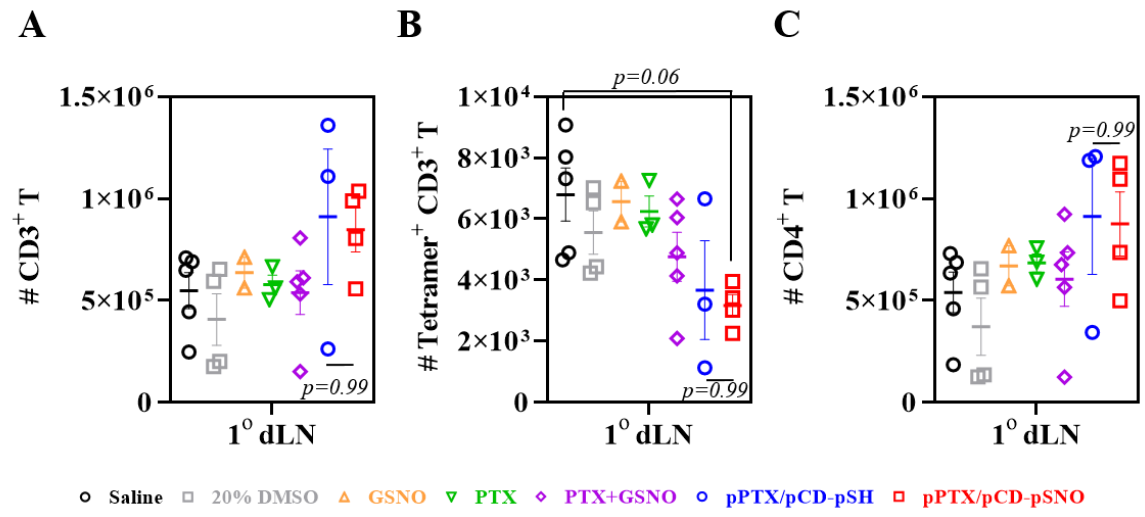

Figure S22. Number profiles of CD3$^+$ T and CD4$^+$ T in 1º dLN. Number of (A) CD45$^+$CD3$^+$ T cells, (B) Tetramer$^+$ CD45$^+$CD3$^+$ T cells, and (C) CD45$^+$CD3$^+$CD4$^+$ T cells in 1º dLN.

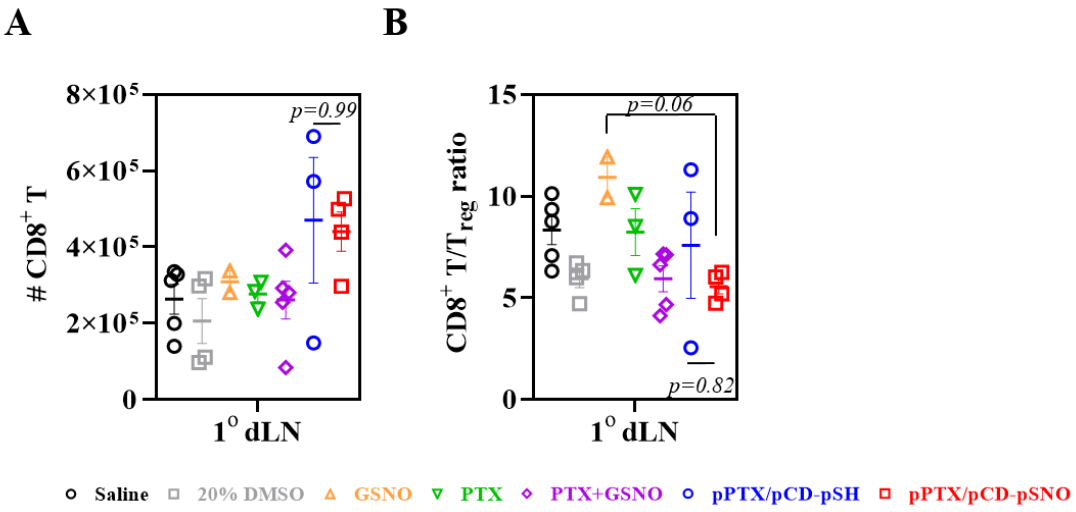

Figure S23. Number profiles of $CD8^+$ T in 1^o dLN. Number of (A) $CD45^+CD3^+CD8^+$ T cells, and (B) ratio of $CD8^+$ T cells to T_{reg} in 1^o dLN.

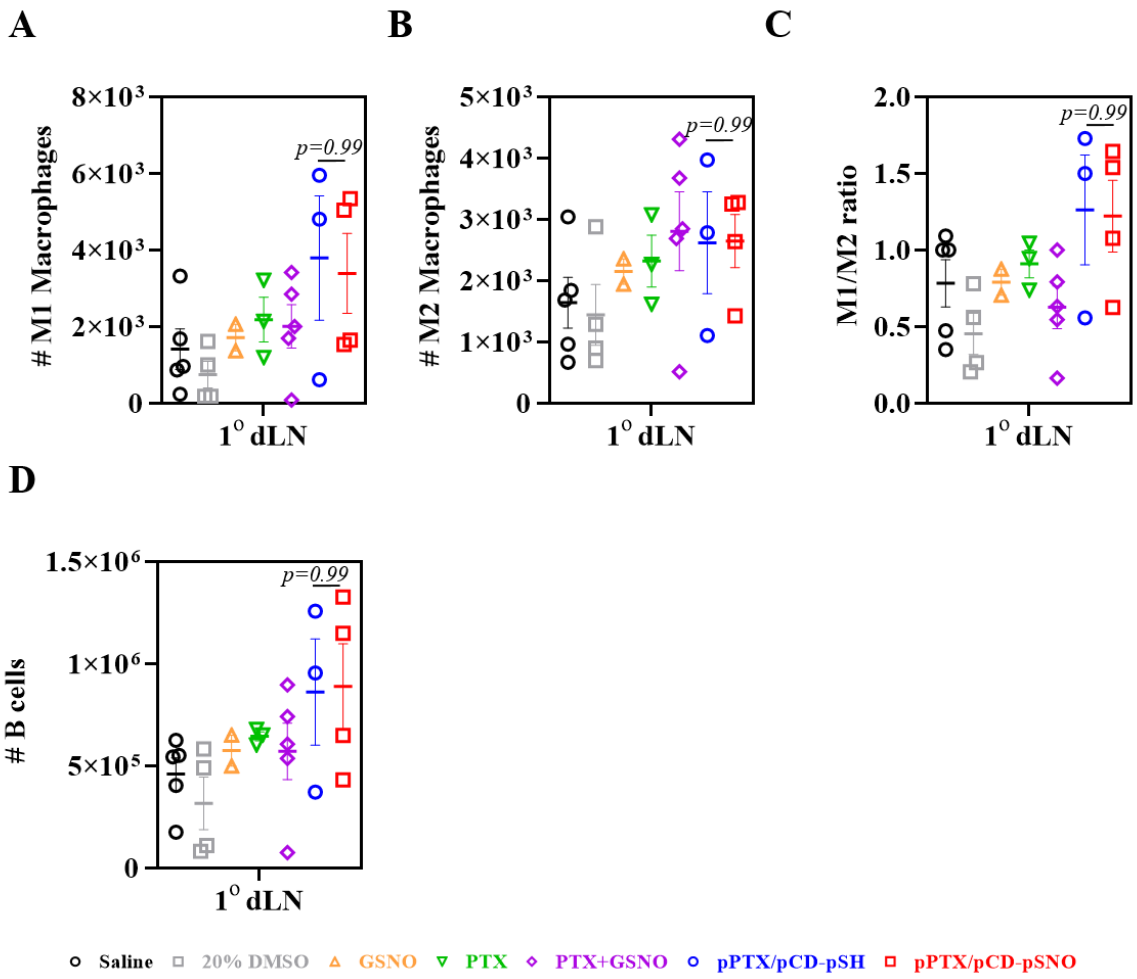

Figure S24. Number profiles of macrophages, and B cells in 1º dLN. Number of (A) $CD45^+CD11b^+F4/80^+CD86^+$ M1 macrophages, (B) $CD45^+CD11b^+F4/80^+CD206^+$ M2 macrophages, (C) ratio of M1 to M2, and (D) $CD45^+CD11b^-B220^+$ B cells in 1º dLN.

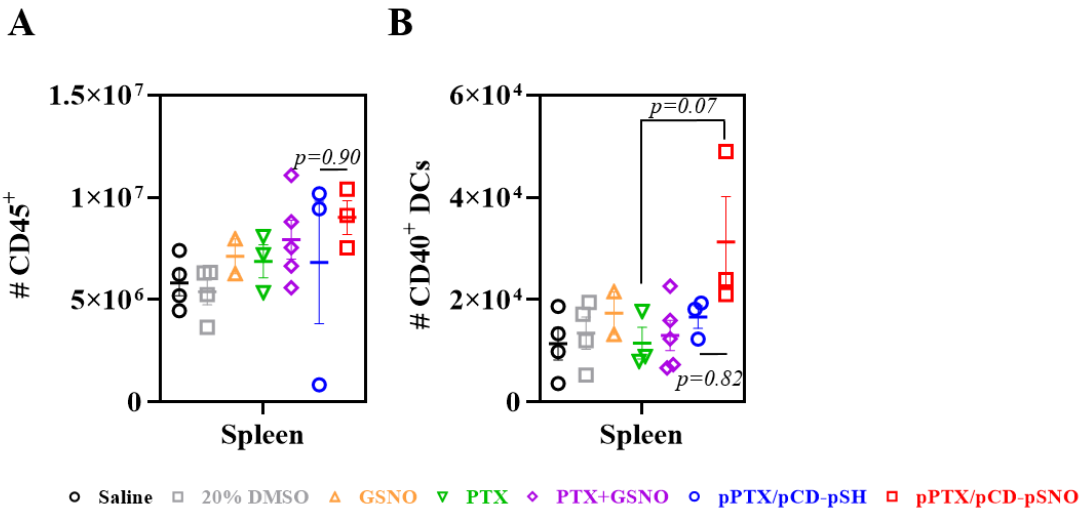

Figure S25. Number profiles of CD45$^+$ cells and DCs in spleen. Number of (A) CD45$^+$ cells, and (B) CD40$^+$ CD45$^+$CD11b$^+$CD11c$^+$ DCs in 1^o spleen.

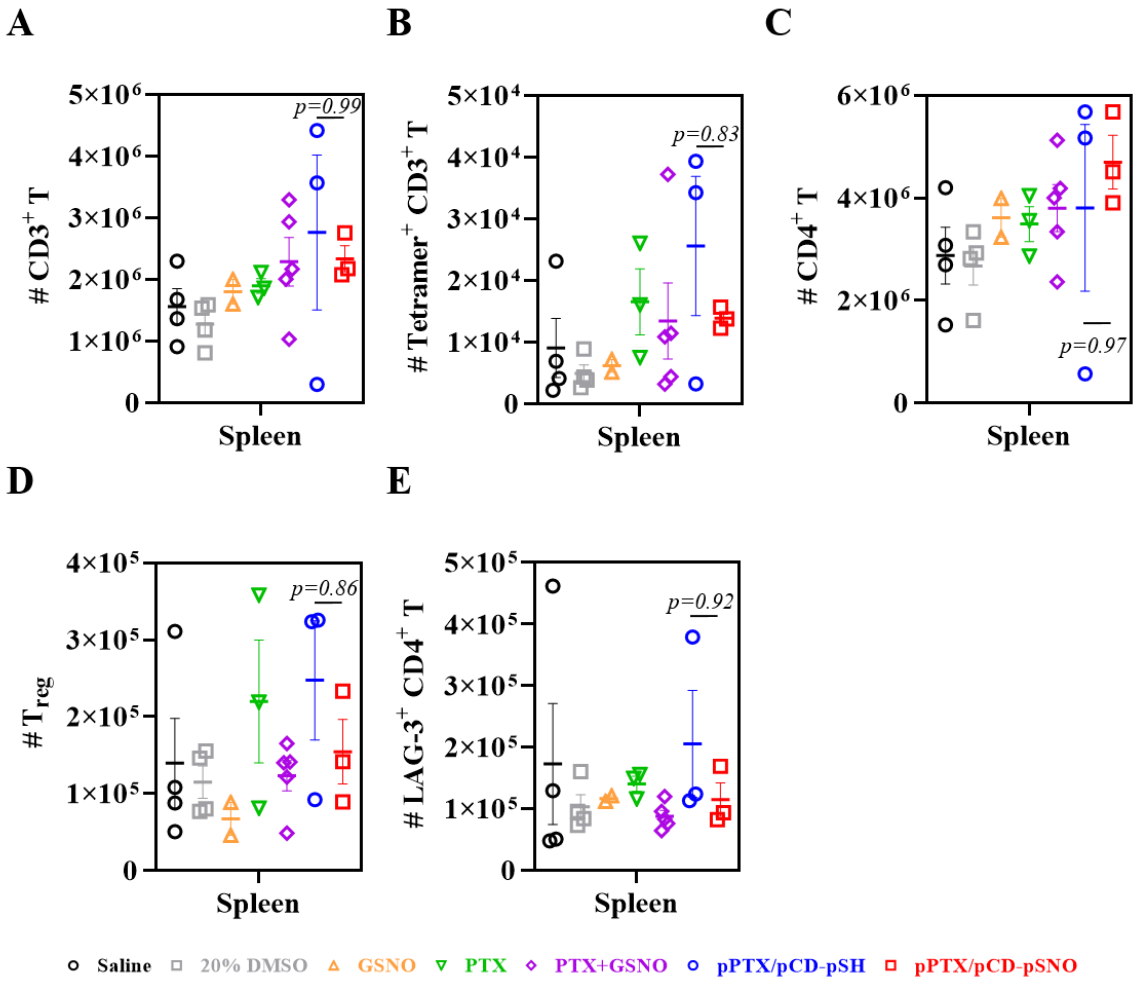

Figure S26. Number profiles of CD3$^+$ T and CD4$^+$ T in spleen. Number of (A) CD45$^+$CD3$^+$ T cells, (B) Tetramer$^+$ CD45$^+$CD3$^+$ T cells, (C) CD45$^+$CD3$^+$CD4$^+$ T cells, (D) CD45$^+$CD3$^+$CD4$^+$CD25$^+$Foxp3$^+$ T_{reg}, and (E) LAG-3$^+$ CD45$^+$CD3$^+$CD4$^+$ T cells in spleen.

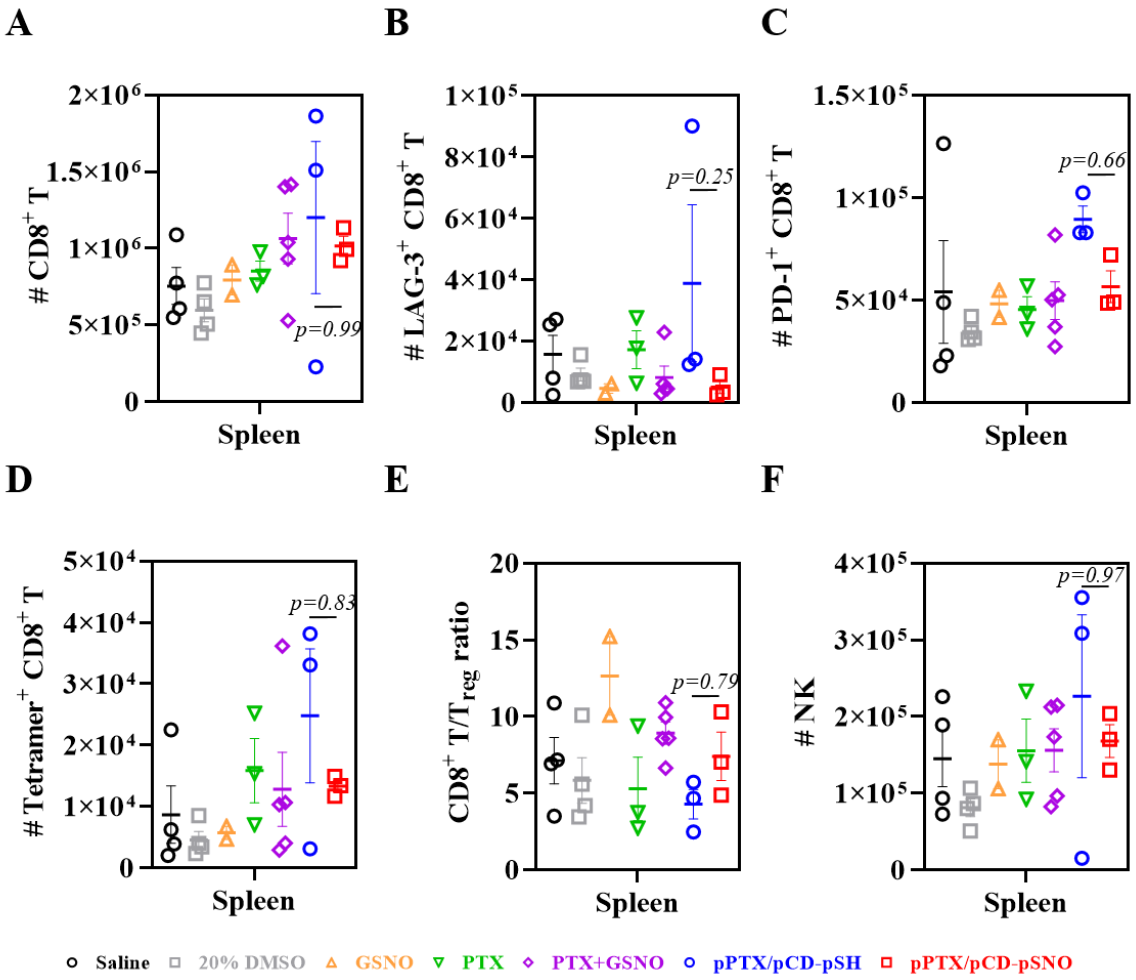

Figure S27. Number profiles of CD8$^+$ T and NK cells in spleen. Number of (A) CD45$^+$CD3$^+$CD8$^+$ T cells, (B) LAG-3$^+$ CD45$^+$CD3$^+$CD8$^+$ T cells, (C) PD-1$^+$ CD45$^+$CD3$^+$CD8$^+$ T cells, (D) Tetramer$^+$ CD45$^+$CD3$^+$CD8$^+$ T cells, (E) ratio of CD8$^+$ T cells to T_{reg}, and (F) CD45$^+$CD3$^-$NK1.1$^+$ NK cells in spleen.

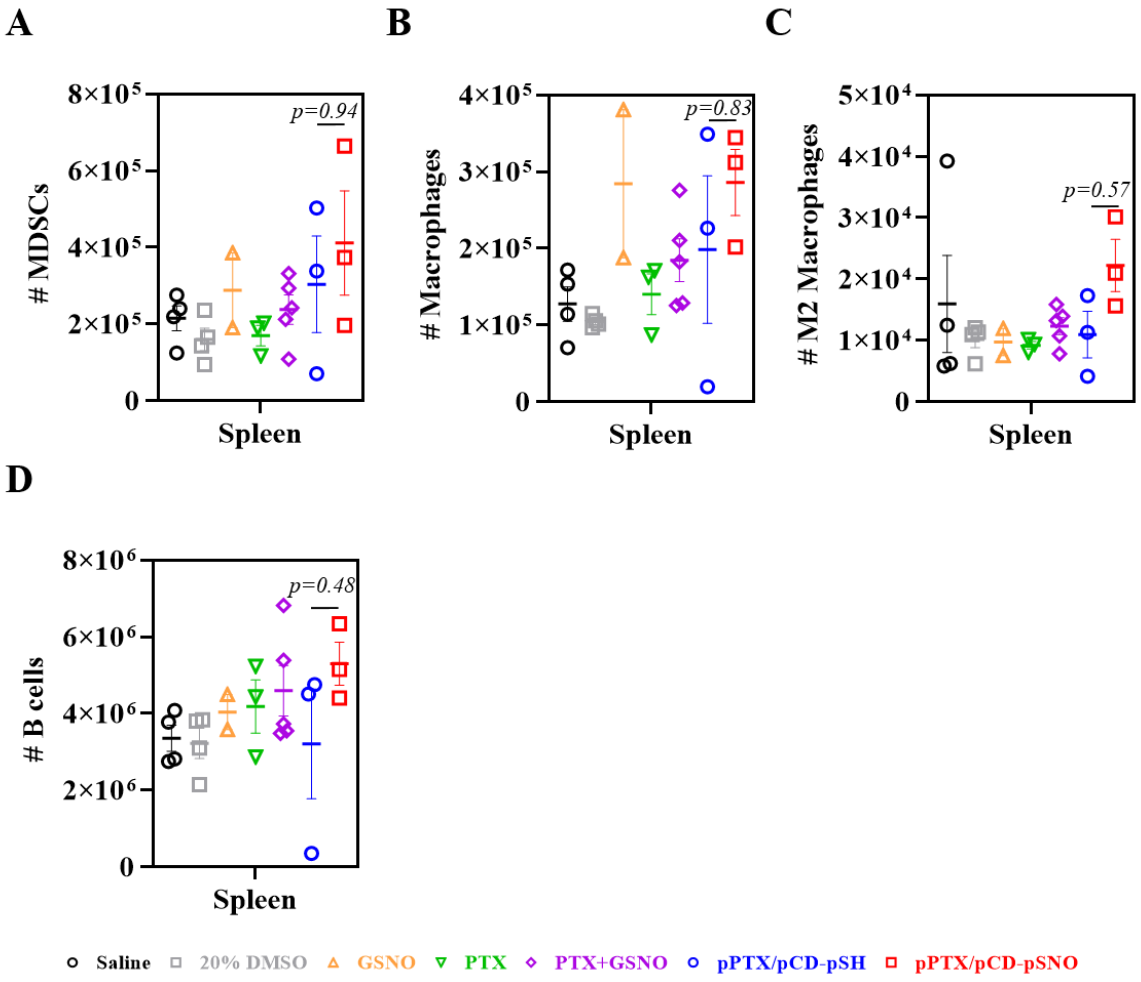

Figure S28. Number profiles of MDSCs, macrophages, and B cells in spleen. Number of (A) $CD45^+CD11b^+CD11c^-Gr1^+$ MDSCs, (B) $CD45^+CD11b^+F4/80^+$ macrophages, (C) $CD45^+CD11b^+F4/80^+CD206^+$ M2 macrophages, and (D) $CD45^+CD11b^-B220^+$ B cells in spleen.

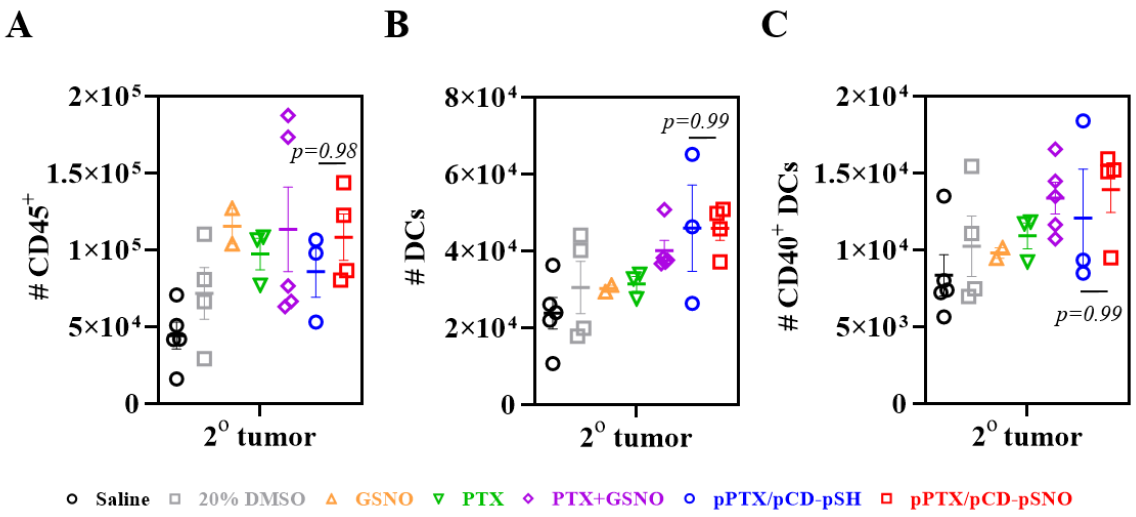

Figure S29. Number profiles of CD45$^+$ cells and DCs in 2^o tumor. Number of (A) CD45$^+$ cells, (B) CD45$^+$CD11b$^+$CD11c$^+$ DCs, and (C) CD40$^+$ CD45$^+$CD11b$^+$CD11c$^+$ DCs in 2^o tumor.

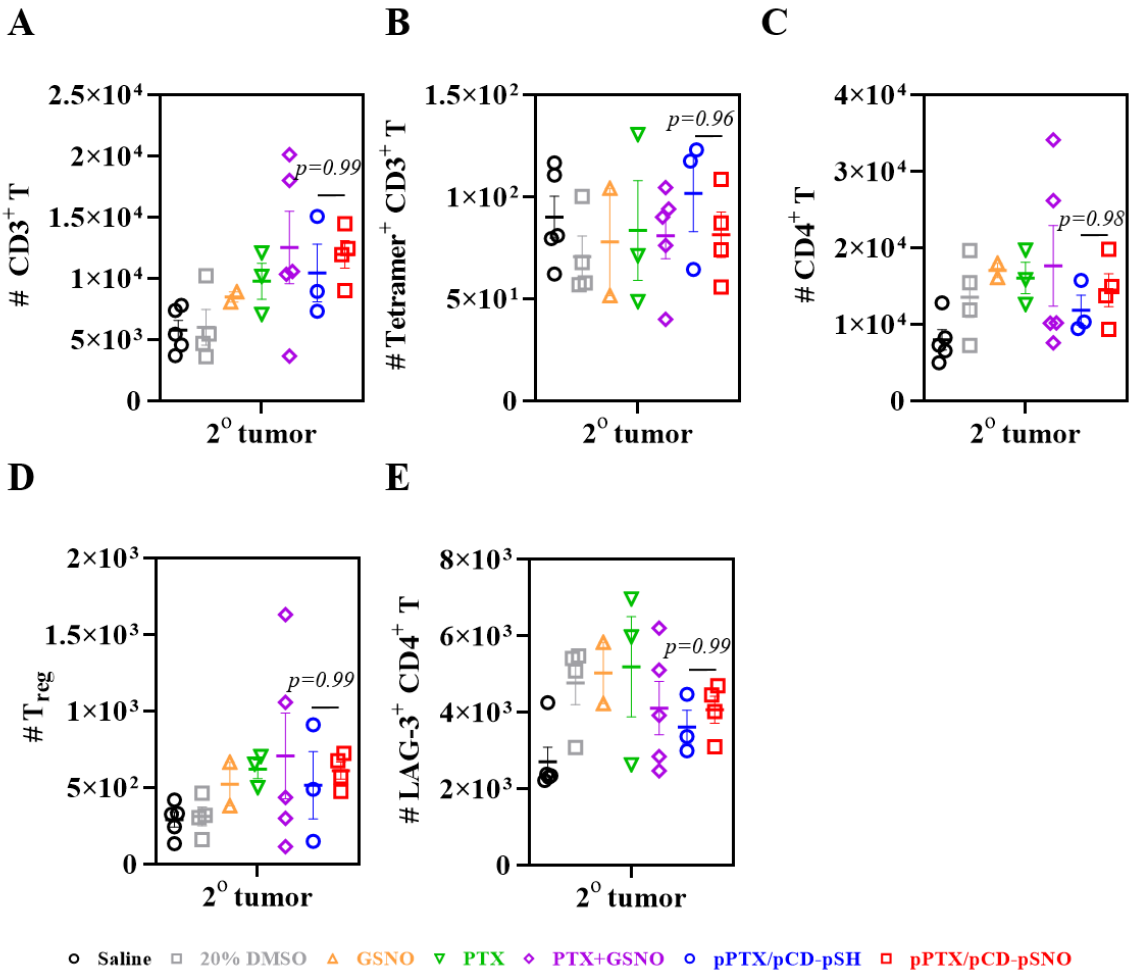

Figure S30. Number profiles of CD3$^+$ T and CD4$^+$ T in 2^o tumor. Number of (A) CD45$^+$CD3$^+$ T cells, (B) Tetramer$^+$ CD45$^+$CD3$^+$ T cells, (C) CD45$^+$CD3$^+$CD4$^+$ T cells, (D) CD45$^+$CD3$^+$CD4$^+$CD25$^+$Foxp3$^+$ T_{reg}, and (E) LAG-3$^+$ CD45$^+$CD3$^+$CD4$^+$ T cells in 2^o tumor.

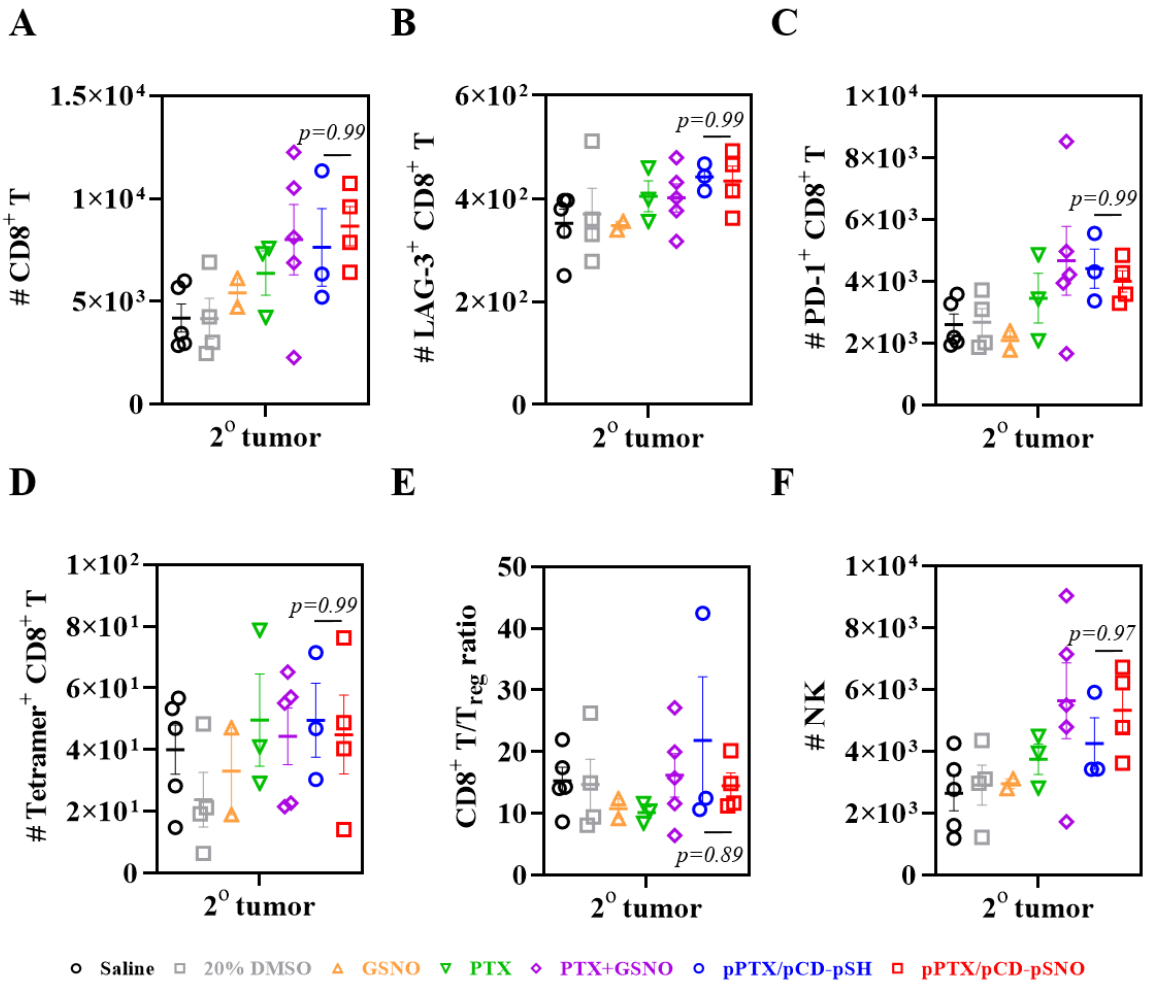

Figure S31. Number profiles of CD8$^+$ T and NK cells in 2^o tumor. Number of (A) CD45$^+$CD3$^+$CD8$^+$ T cells, (B) LAG-3$^+$ CD45$^+$CD3$^+$CD8$^+$ T cells, (C) PD-1$^+$ CD45$^+$CD3$^+$CD8$^+$ T cells, (D) Tetramer$^+$ CD45$^+$CD3$^+$CD8$^+$ T cells, (E) ratio of CD8$^+$ T cells to T_{reg}, and (F) CD45$^+$CD3$^-$NK1.1$^+$ NK cells in 2^o tumor.

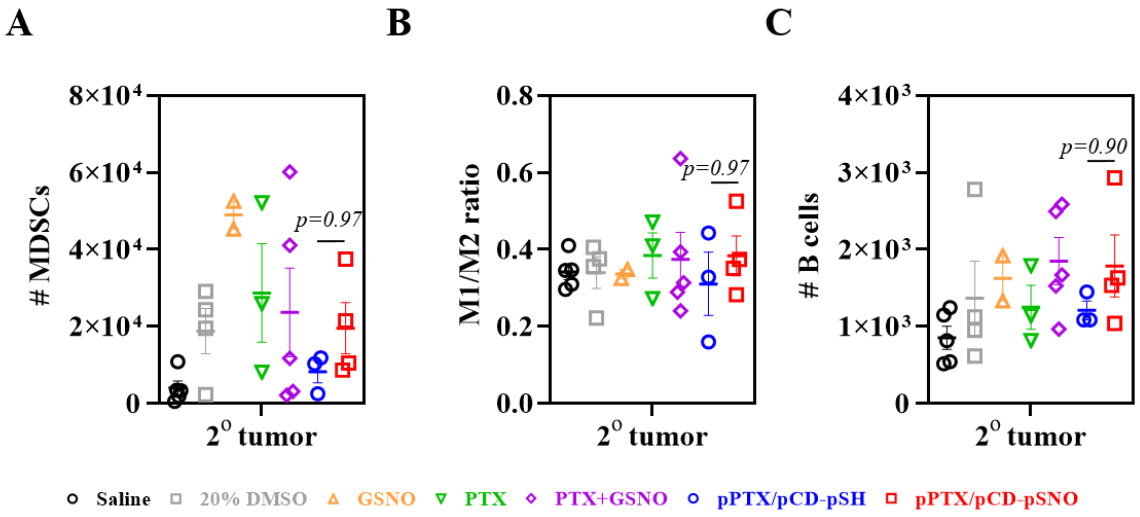

Figure S32. Number profiles of MDSCs, macrophages, and B cells in 2º tumor. Number of (A) $CD45^{+}CD11b^{+}CD11c^{-}Gr1^{+}$ MDSCs, (B) ratio of M1 to M2, and (C) $CD45^{+}CD11b^{-}B220^{+}$ B cells in 2º tumor.

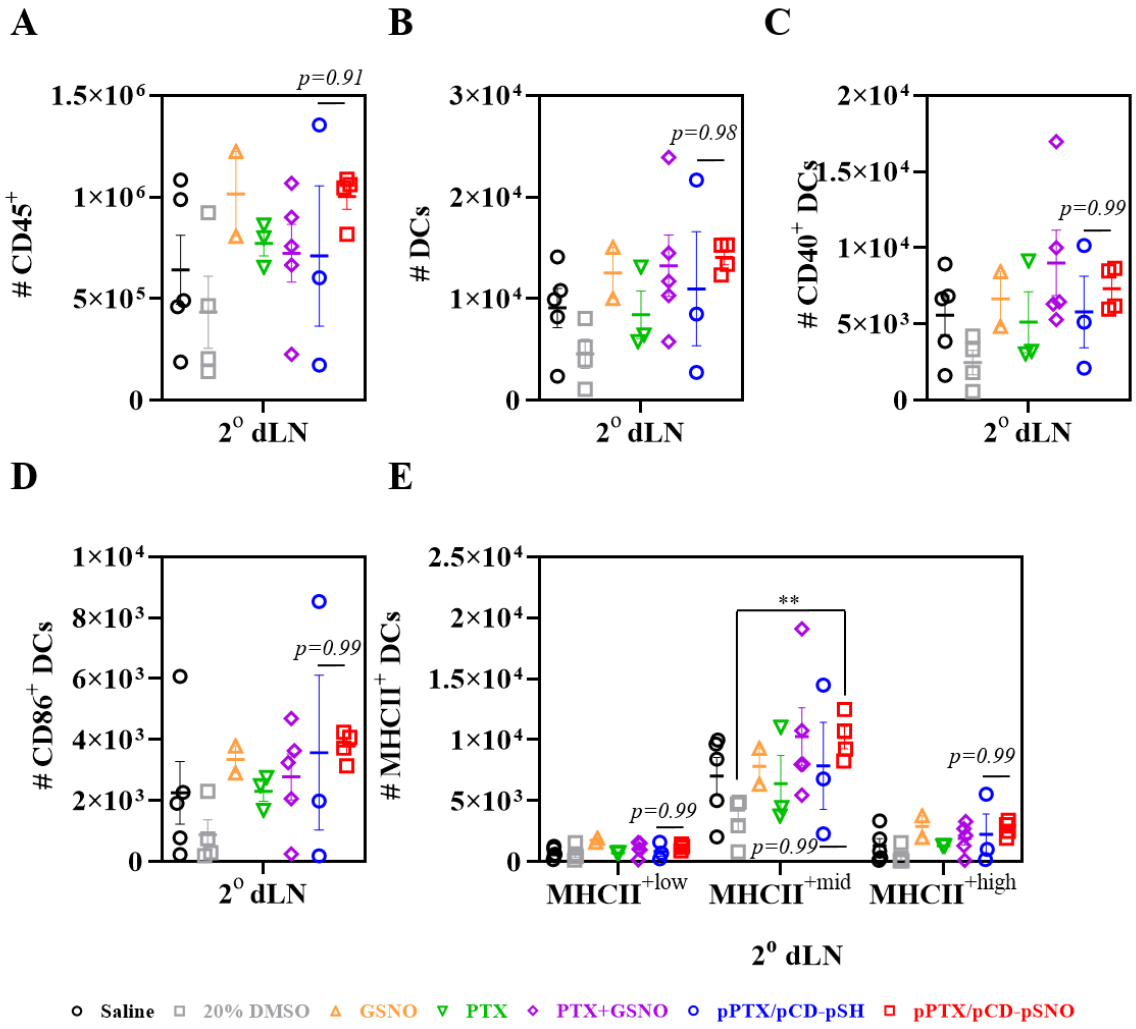

Figure S33. Number profiles of CD45$^+$ cells and DCs in 2º dLN. Number of (A) CD45$^+$ cells, (B) CD45$^+$CD11b$^+$CD11c$^+$ DCs, (C) CD40$^+$ CD45$^+$CD11b$^+$CD11c$^+$ DCs, (D) CD86$^+$ CD45$^+$CD11b$^+$CD11c$^+$ DCs, (E) MHCII^{+low}, MHCII^{+mid}, and MHCII^{+high} CD45$^+$CD11b$^+$CD11c$^+$ DCs in 2º dLN.

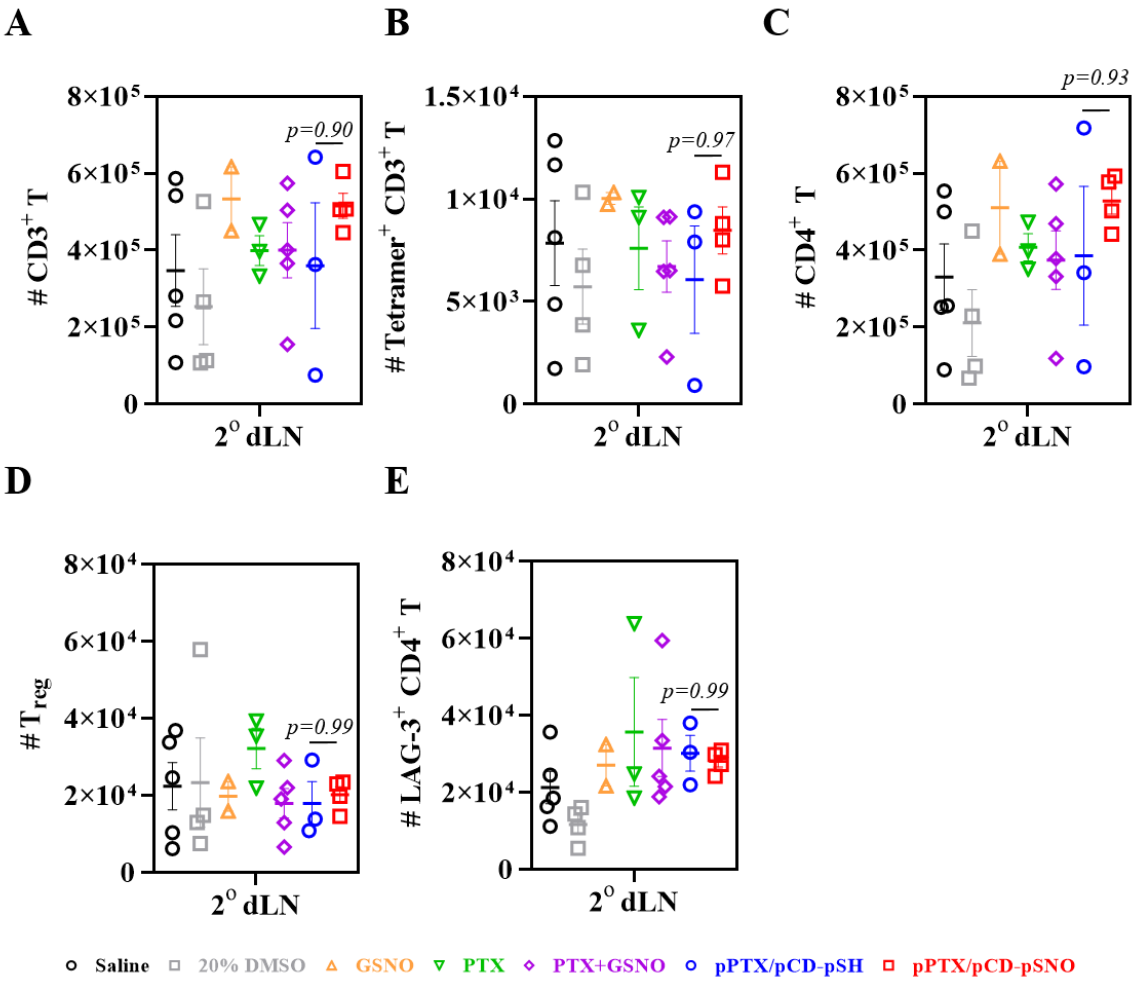

Figure S34. Number profiles of $CD3^+$ T and $CD4^+$ T in 2^o dLN. Number of (A) $CD45^+CD3^+$ T cells, (B) $Tetramer^+$ $CD45^+CD3^+$ T cells, (C) $CD45^+CD3^+CD4^+$ T cells, (D) $CD45^+CD3^+CD4^+CD25^+Foxp3^+$ T_{reg}, and (E) LAG-3^+ $CD45^+CD3^+CD4^+$ T cells in 2^o dLN.

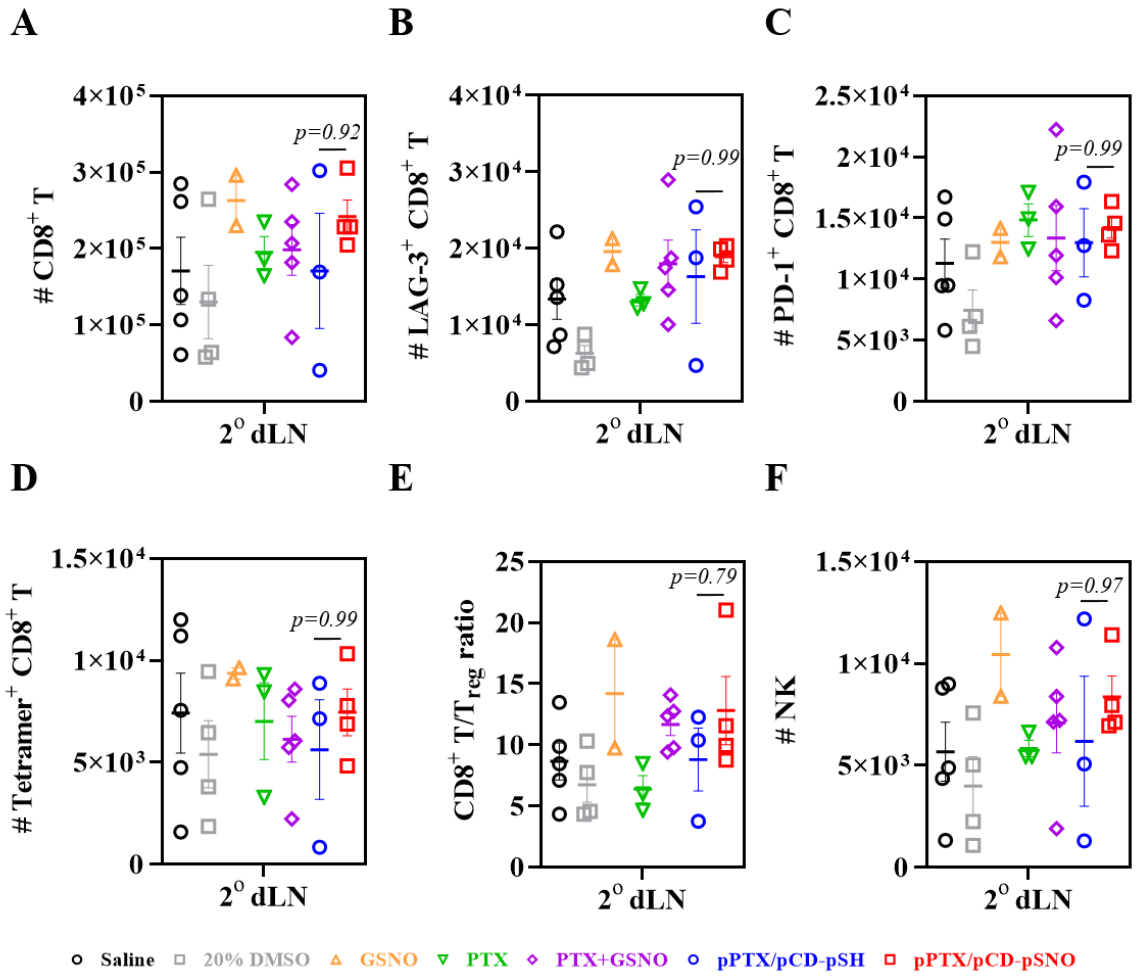

Figure S35. Number profiles of CD8$^+$ T and NK cells in 2^o dLN. Number of (A) CD45$^+$CD3$^+$CD8$^+$ T cells, (B) LAG-3$^+$ CD45$^+$CD3$^+$CD8$^+$ T cells, (C) PD-1$^+$ CD45$^+$CD3$^+$CD8$^+$ T cells, (D) Tetramer$^+$ CD45$^+$CD3$^+$CD8$^+$ T cells, (E) ratio of CD8$^+$ T cells to T_{reg}, and (F) CD45$^+$CD3$^-$NK1.1$^+$ NK cells in 2^o dLN.

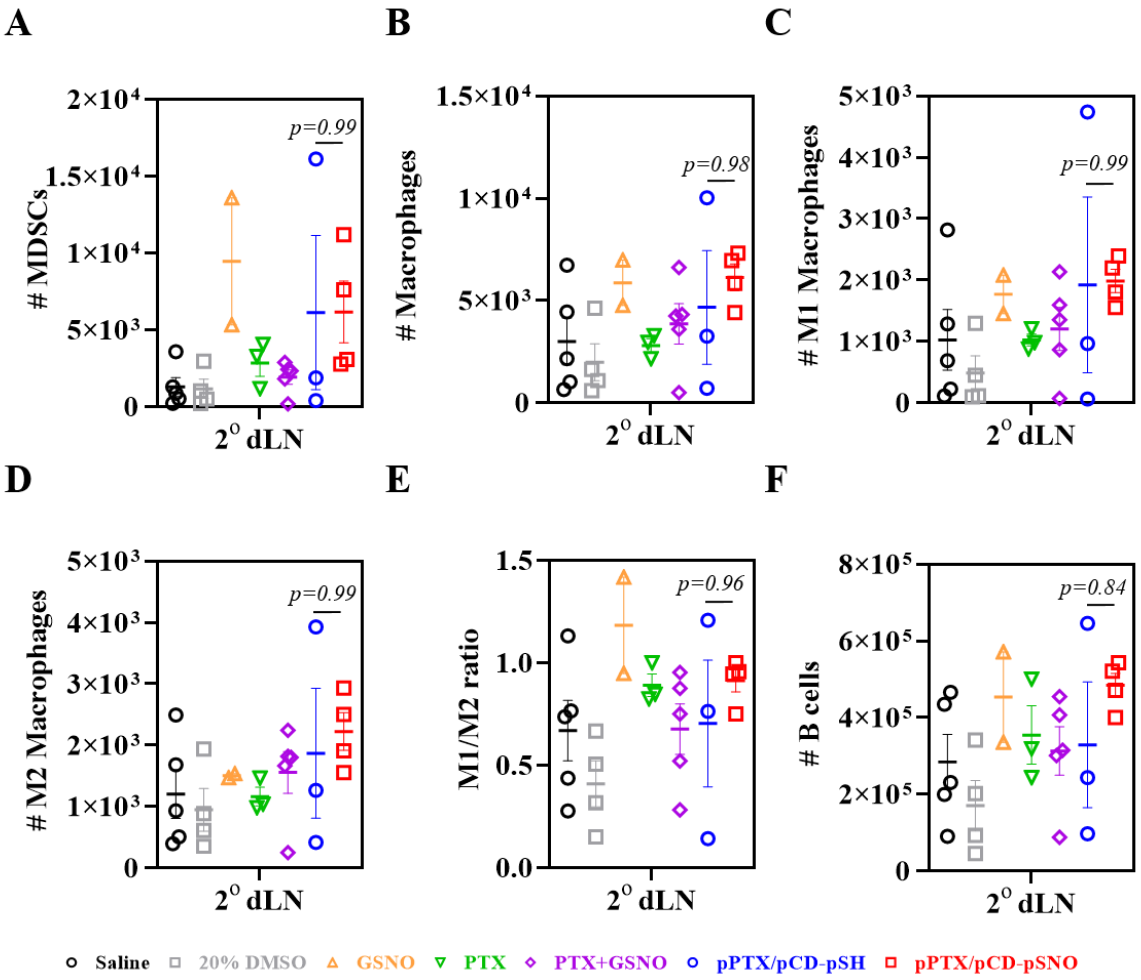

Figure S36. Number profiles of macrophages, and B cells in 2º dLN. Number of (A) $CD45^+CD11b^+CD11c^-Gr1^+$ MDSCs, (B) $CD45^+CD11b^+F4/80^+$ macrophages, (C) $CD45^+CD11b^+F4/80^+CD86^+$ M1 macrophages, (D) $CD45^+CD11b^+F4/80^+CD206^+$ M2 macrophages, (E) ratio of M1 to M2, and (F) $CD45^+CD11b^-B220^+$ B cells in 2º dLN.